Lichttechnisches Institut (LTI)
UNIVERSITÄT KARLSRUHE

Nanostructures for Surface Plasmon enhanced light emission

Mònica Alfonso Larrégola

September 2008

Supervisor:
MSc. Yousef Nazirizadeh

I declare that this work has been composed by me, and is a record of work done by me, and has not previously been presented for a higher degree. This project was concluded by me at the University of Karlsruhe, Germany, from April to September 2008.

Karlsruhe, 11 September 2008
Mònica Alfonso

Contents

0 Resum en català

Introducció

L'emissió espontània juga un paper important a dispositius com els LEDs o els làsers. És important saber manipular l'emissió espontània per tal de millorar el funcionament d'aquests dispositius. Podem manipular-la de dues formes diferents: augmentant-la o inhibint-la. Per exemple, augmentar l'emissió espontània a la cavitat d'un làser en la direcció de la cavitat permet disminuir el llindar, quan el làser passa d'emissió espontània a emissió estimulada. Una de les aplicacions més populars de la manipulació de l'emissió espontània és l'augment de l'emissió als LEDs. Es pot manipular l'emissió espontània de diverses maneres com amb l'ús de microcavitats o amb polaritons plasmònics superficials. Aquest darrer mètode és el que es farà servir.

Emissió espontània

L'emissió espontània és l'emissió d'un fotó per un àtom, amb la transició de l'àtom d'un estat electrònic E_2 a un estat d'energia inferior E_1. Hi ha dos tipus d'emissió espontània: fosforescència i fluorescència. En el nostre cas, es tractarà d'augmentar l'emissió espontània amb l'excitació dels polaritons plasmònics superficials produïda per unes molècules fluorescents. El procés de fluorescència es mostra a la figura 1:

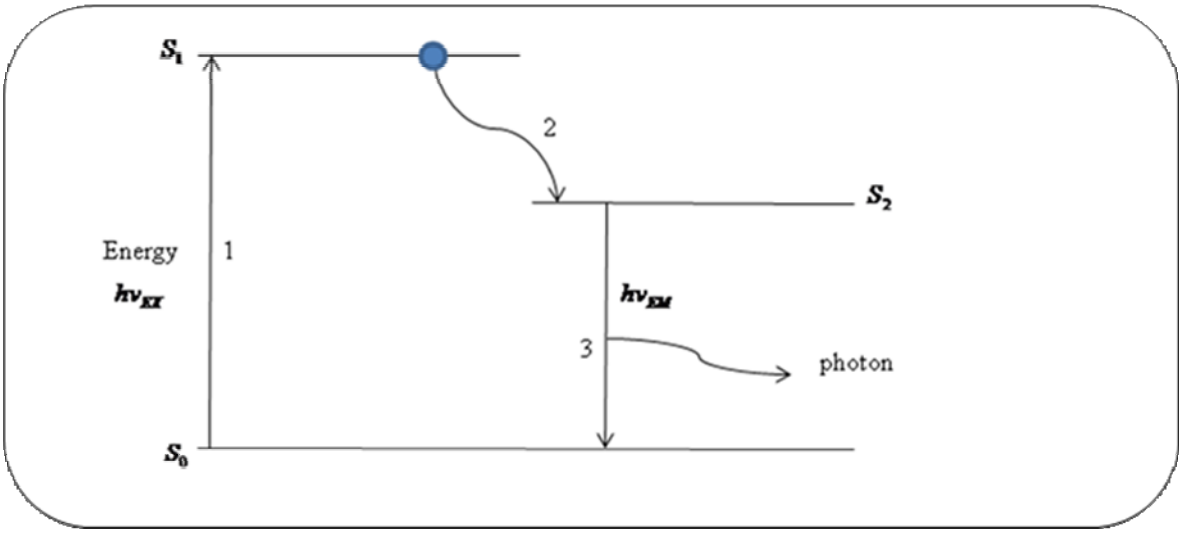

Figura 1. Procés de fluorescència

Un àtom és excitat a un nivell d'energia prohibit S_1, després d'un cert temps, decau a un nivell d'energia permès S_2 des d'on torna al nivell inicial d'energia emetent llum. El nivell d'energia S_2 és menor que el nivell S_1, així doncs, la longitud d'ona del fotó emès és major que la de l'excitació.

La intensitat de la fluorescència que es pot generar es pot saber a partir de l'estudi de l'espectre d'emissió com el que es pot veure a la figura 2:

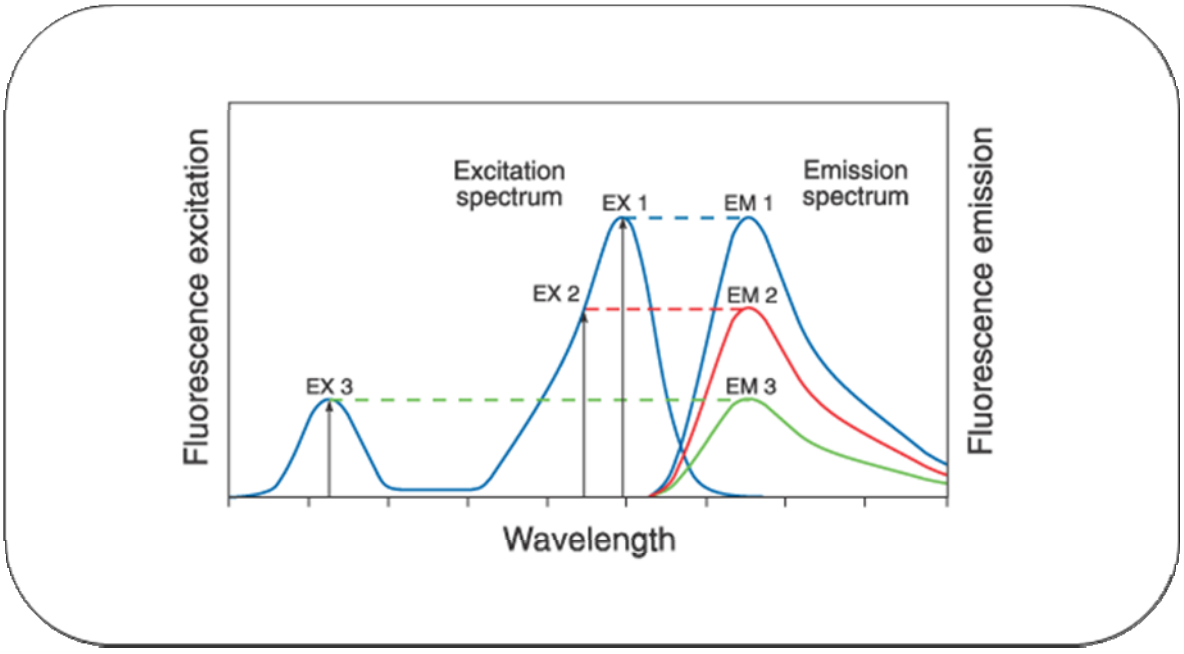

Figura 2: Espectre de fluorescència [10].

La longitud d'ona de l'emissió no depèn de la longitud d'ona de l'excitació. La única cosa que varia en funció de l'excitació és l'amplitud de l'emissió.

Tornant al tema de l'emissió espontània, si tenim N àtoms a l'estat alt, N decaurà seguint l'expressió:

$$\frac{\partial N}{\partial t} = -A_{rad} N$$

On A_{rad} és el ràtio de l'emissió espontània (A coeficient d'Einstein). L'equació pot ser resolta com:

$$N(t) = N(0)e^{-A_{rad}t}$$

On $N(0)$ és el nombre inicial d'àtoms a l'estat excitat i A_{rad} és el ràtio de caiguda radiativa de la transmissió. A_{rad} és inversament proporcional al temps de vida τ_{rad}:

$$A_{rad} = \frac{1}{\tau_{rad}}$$

Polaritons plasmònics superficials

Els polaritons plasmònics superficial són modes electromagnètic constituïts per un camp lluminós acoblat a una oscil·lació col·lectiva d'electrons propagant-se a la interfície entre un metall i un dielèctric. El seu camp elèctric té un màxim a la superfície i decau exponencialment seguint en la direcció perpendicular a la superfície, com es pot veure a la figura 3:

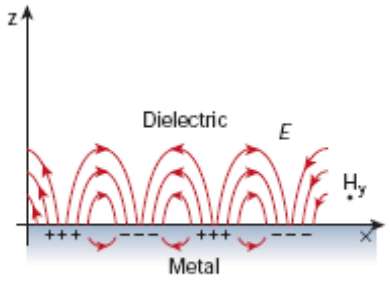

Figura 3: Camp electromagnètic degut als polaritons plasmònics superficial [15].

Quan els emissors localitzats prop d'una superfície metàl·lica decauen mitjançant emissió espontània ho poden fer de tres maneres diferents: com a radiació útil, com a polaritons plasmònics superficials i com a pèrdues al metall. Els polaritons plasmònics superficials i les pèrdues al metall són processos no radiatius. Entre els polaritons plasmònics superficials i la llum visible hi ha una diferència de moments. Per tant, si es pogués extreure l'energia perduda als polaritons plasmònics superficials com a radiació, augmentaríem l'emissió espontània. S'ha demostrat que l'emissió espontània dels polaritons plasmònics superficials és més forta que la llum emesa directament, cosa que també contribueix a l'augment de l'emissió espontània.

Resolent les equacions de Maxwell amb les condicions de contorn adequades, s'obté el vector d'ona del polaritó plasmons superficial, k_{SP} :

$$k_{SP} = k_0 \sqrt{\frac{\varepsilon_d \varepsilon_m}{\varepsilon_d + \varepsilon_m}}$$

On ε_d i ε_m són les permitivitats relatives del dielèctric i del metall, respectivament; i $k_0 = \omega / c$ és el vector d'ona de l'espai lliure.

A la corba de dispersió d'un polaritó plasmons superficial es pot veure la diferencia de moments existent entre la llum i el polaritó plasmons superficial. Es pot observar a la figura 4:

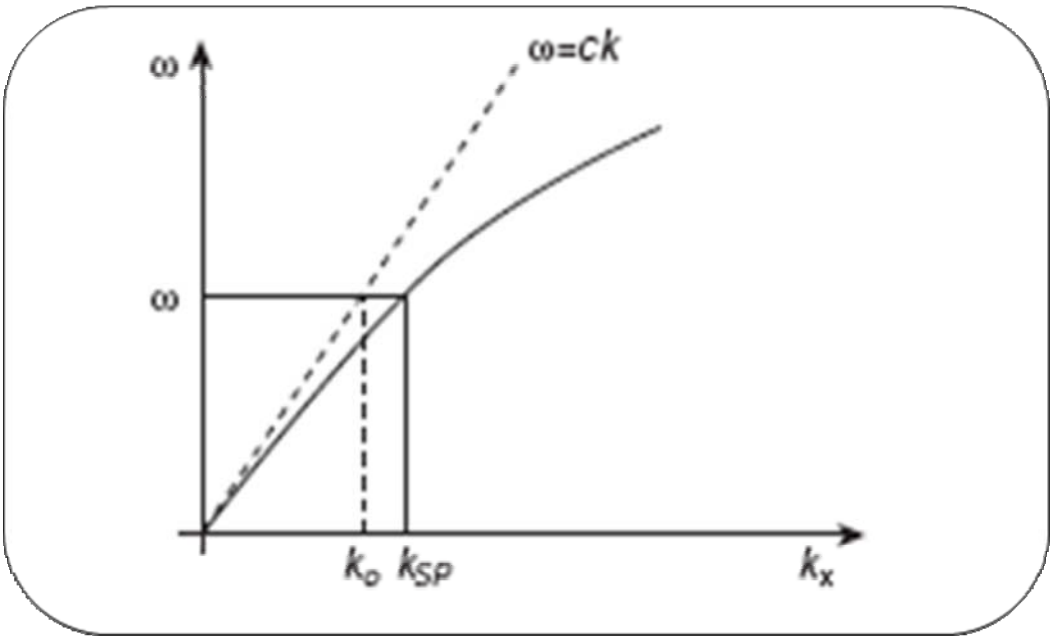

Figura 4: Corba de dispersió d'un polaritó plasmons superficial [15].

La conversió dels polaritons plasmònics superficials en llum es pot fer mitjançant diverses tècniques com l'ús d'una reixa periòdica a la superfície del metall o l'ús de la pròpia rugositat del metall. Aquest últim cas és el que s'estudiarà.

Rugositat

La rugositat d'un material és definida per les desviacions verticals de la superfície del material respecte la seva forma ideal.

En la mesura de la rugositat d'un material hi ha *n* punts equitativament espaiats. Y_i és la distancia vertical entre un punt de dades i l'alçada mitja. Un paràmetre per definir la rugositat és el següent, on R_p i R_v són les alçades dels punts màxim i mínim de la superfície, respectivament:

$$R_{RMS} = \sqrt{\frac{1}{n}\sum_{i=1}^{n} y_i^2}$$

Teoria de Mie

La teoria de Mie defineix una solució per a la intensitat de dispersió d'una esfera isotròpica en un medi homogeni. Podem diferenciar entre dos fenòmens diferents depenent de la relació entre la mida de l'esfera i la longitud d'ona incident. Es tracta de dispersió de Rayleigh quan la mida de la partícula és menor que la longitud d'ona de la llum i dispersió de Mie quan la mida de la partícula és comparable a la longitud d'ona incident. En el nostre experiment es produeix dispersió de Rayleigh. En la dispersió de Rayleigh la intensitat de la dispersió depèn de la longitud d'ona de la llum segons la següent equació:

$$I \propto \left(\frac{a}{\lambda}\right)^4$$

On *a* és el radi de la partícula. Aquesta intensitat és major per longituds d'ona menors.

S'ha demostrat que la superfície d'un material es pot modelar com si es tractés de petites esferes de diàmetre l'alçada del perfil. Seguint aquest raonament, es pot aplicar la teoria de Mie al nostre experiment.

Fabricació de les mostres

Les mostres estudiades segueixen el següent esquema:

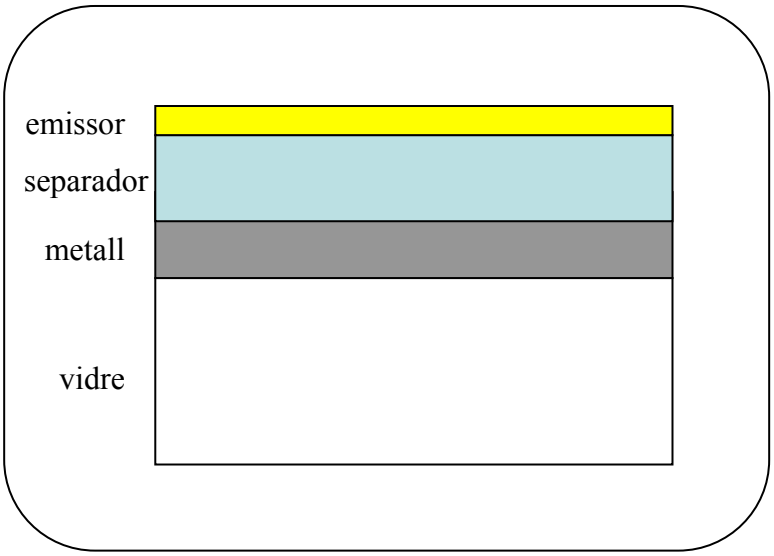

Figura 5. Geometria de la mostra

Sobre un substrat de vidre s'ha dipositat una capa de metall de 50 nm de gruix mitjançant una tècnica d'evaporació tèrmica. Es comparen dos metalls diferents: or i plata. Per això, després de dipositar la capa de metall, s'estudia la seva superfície amb un microscopi de força atòmica. Es veu que la plata presenta una rugositat major i, per tant, hauria de ser millor que l'or per a aquest experiment.

Com més a prop es doni l'emissió de la capa metàl·lica, millor acoblament es donarà entre la llum emesa i els polaritons plasmònics superficials. Tot i això, es col·loca un separador entre l'emissor i el metall per tal d'evitar que es produeixin reaccions químiques entre l'emissor i el metall i per tal d'evitar que es perdi gran quantitat de potencia al metall. Es comparen dos tipus de separadors de diferents gruixos: PMMA (polimetil metacrilat) i Ta_2O_5 (pentòxid de tàntal). El PMMA és dipositat al metall amb *spin-coating*. Es troben dificultats per arribar a gruixos petits i es decideix descartar l'ús d'aquest material com a separador. Aleshores es dipositen capes de 10, 45 i 100 nm de gruix mitjançant evaporació tèrmica. S'espera obtenir els millors resultats pels menors gruixos de separador.

Per últim, també es compararà l'efecte d'emissors amb diferents freqüències d'emissió. L'emissor usat és FluoSpheres®, subministrat per Molecular Probes, amb màximes freqüències d'absorció/emissió a 505/515, 540/560 i 580/605 nm. És dipositat sobre la capa separadora per *spin-coating*.

Mesures

Per mesurar la fotoluminescència es va fer el següent: la mostra es col·loca sobre un suport i és excitada per la seva cara frontal des d'un angle de 45º per un làser de 400 nm. La seva emissió (també per la cara frontal) és recollida per una fibra òptica. L'ona resultant és processada per un monocromador i una càmera CCD. El sistema muntat es mostra a la figura 6.

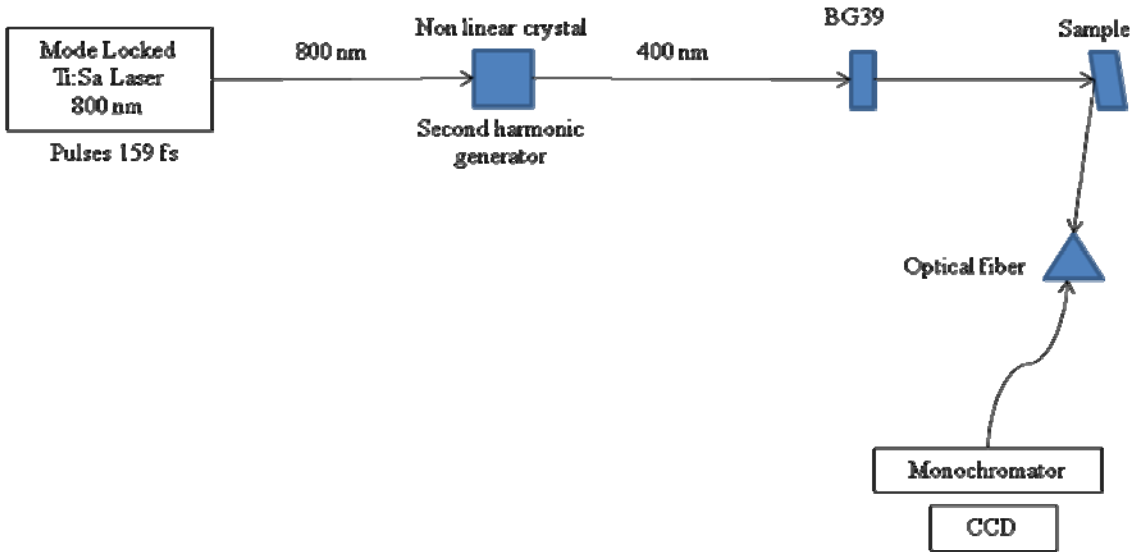

Figura 6. Muntatge per la mesura de la fotoluminescència

S'obté l'espectre que mostra la figura 7. La fotoluminescència s'ha vist multiplicada per 5,4 per a la plata.

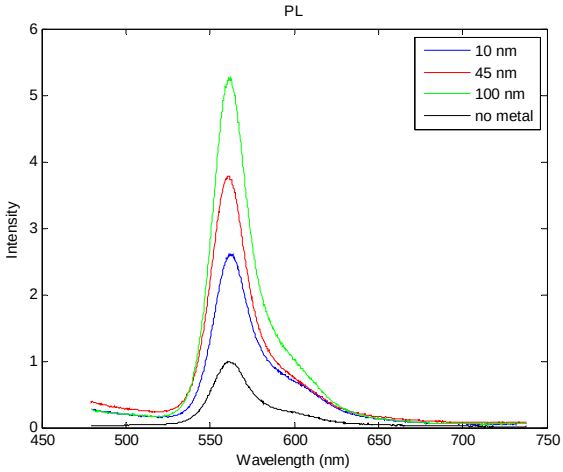

Figura 7. Intensitat de fotoluminescència per a mostres de plata amb un emissor de 560 nm. Es comparen diferents gruixos de separadors.

A les figures 8 i 9 es veu el ràtio d'augment de la fotoluminescència per a mostres d'or i plata amb un emissor de 560 nm.

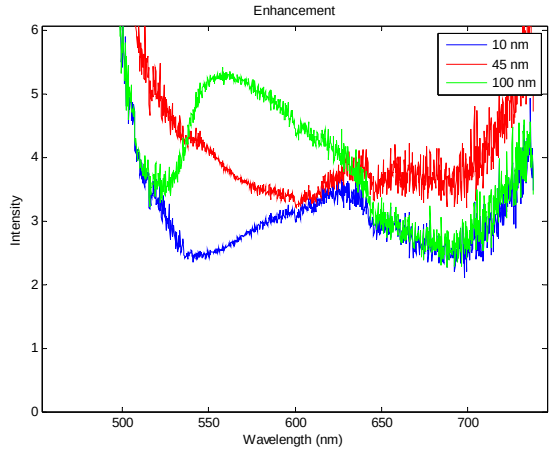

Figura 8. Ràtio d'augment de la fotoluminescència per mostres de plata amb un emissor de 560 nm. Es comparen diferents gruixos de separador.

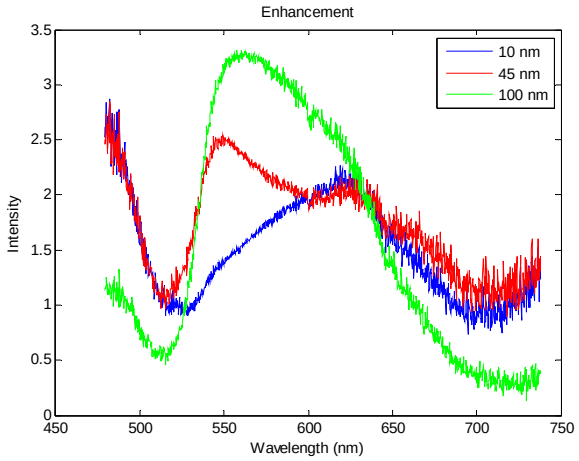

Figura 9. Ràtio d'augment de la fotoluminescència per mostres d'or amb un emissor de 560 nm. Es comparen diferents gruixos de separador.

Les freqüències de plasma per a l'or i la plata es troben a 650 nm i 558 nm, respectivament. Les emissions de les fluorosferes es troben a 515 nm, 560 nm i 605 nm. Com més a prop es trobi l'emissió de la freqüència de plasma, millor serà l'acoblament que presentarà als polaritons plasmònics superficials. Així, s'espera que el millor acoblament entre la llum i els polaritons plasmònics superficials es doni amb l'emissor de 605 nm per a l'or i amb l'emissor de 560 nm per la plata.

Es pot veure com el ràtio d'augment de la fotoluminescència de les figures 8 i 9 és molt similar, tot i que es presenta un major augment per la plata. A partir d'això, es pot deduir que la millora observada no és deguda als polaritons plasmònics superficials. Si fós deguda a això, s'observaria una diferència entre els 2 metalls, ja que es comporten de manera diferent amb la longitud d'ona.

Es pensa que els resultats obtinguts són deguts a efectes de la capa metàl·lica, que causen interferències a l'espectre de fotoluminescència. La diferència entre l'augment de la fotoluminescència observat per a l'or i la plata és degut a la reflexió sobre el metall de les ones emeses per les fluorosferes. La longitud d'ona de plasma de la plata es troba a 558 nm i la longitud d'ona de plasma de l'or es troba a 650 nm. La llum de freqüència superior a la freqüència de plasma és transmesa, mentre que la llum de freqüència inferior a la freqüència de plasma és reflexada. Per aquest motiu, la quantitat de llum reflectida és major per a la plata que per a l'or, cosa que repercuteix en la mesura de la fotoluminescència.

Per entendre millor aquest comportament, es decideix estudiar el temps de vida de la fotoluminescència. El temps de vida de la fotoluminescència és inversament proporcional al ràtio de l'emissió espontània. El sistema muntat per la realització de les mesures es mostra a la figura 10. Els resultats obtinguts es mostren a les figures11 i 12 amb eixos semi logarítmics.

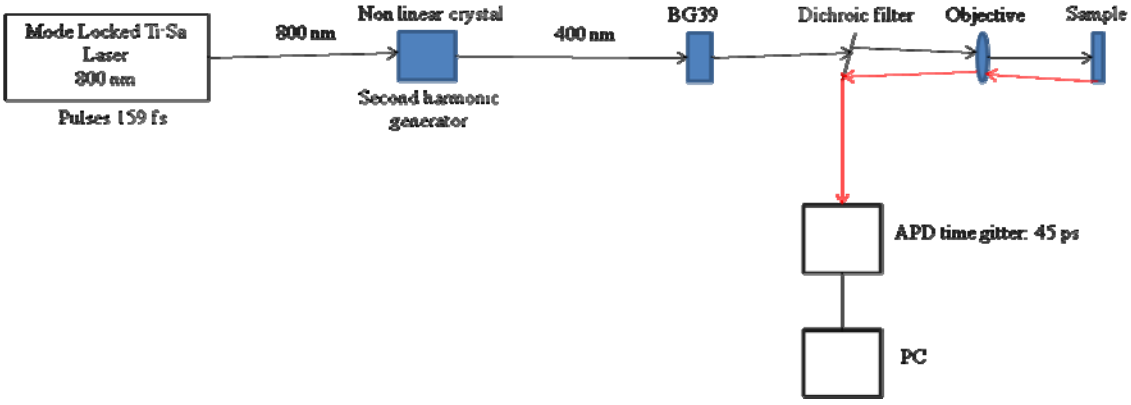

Figura 10. Muntatge per a la mesura del temps de vida de la fotoluminescència.

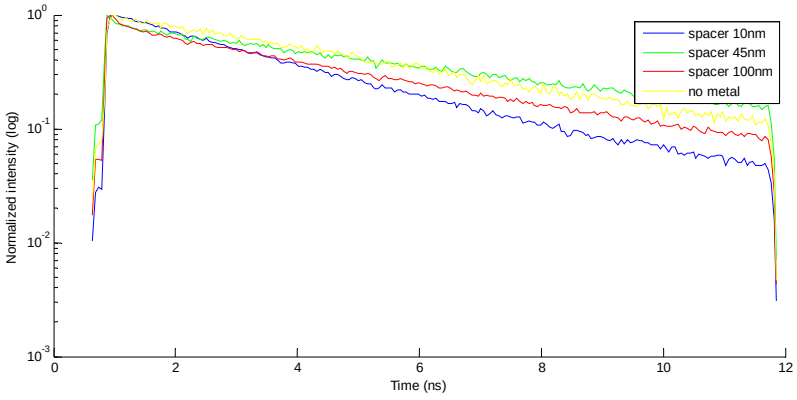

Figura 11. Temps de vida de la fotoluminescència per mostres de plata amb un emissor de 560 nm. Es comparen diferents gruixos de separadors.

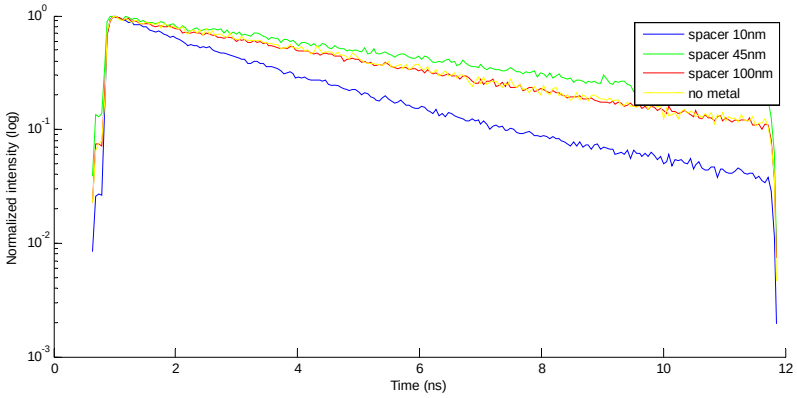

Figura 12. Temps de vida de la fotoluminescència per mostres d'or amb un emissor de 560 nm. Es comparen diferents gruixos de separadors.

S'observa com per ambdós metalls el temps de vida menor es dóna per un gruix del separador de 10 nm, el que es correspon amb un elevat ràtio d'augment de l'emissió espontània, tal com preveu la teoria. De totes maneres, s'observa un temps de vida de la fotoluminescència menor per a mostres amb un separador de 100 nm que per a mostres amb un separador de 45 nm, cosa que es contradiu amb els resultats previstos. Com succeïa amb les mesures de la fotoluminescència, es creu que aquest comportament és degut a reflexions al metall. Els resultats han estat corroborats més tard amb la realització de simulacions amb el software Lumerical.

Una raó que explica l'inesperat comportament de les mostres és l'existència d'interferències entre les ones emeses directament i les ones reflectides al metall. Un altre fet important que afecta la mesura de la fotoluminescència és la pèrdua d'energia al metall, que depèn de la longitud d'ona de l'emissió i del gruix de la capa separadora. Així doncs, la fotoluminescència mesurada depèn de la pròpia emissió de les fluorosferes deguda a l'excitació del làser i la reflexió al metall de l'emissió de les fluorosferes i del làser.

Conclusió

S'ha observat un augment en la fotoluminescència per mostres cobertes de metall, amb un emissor separat del metall per una capa separadora. L'acoblament als polaritons plasmònics superficials és major quan menor és la distància entre l'emissió i

el metall. Així doncs, s'hauria d'observar un augment de la fotoluminescència major per a gruixos de separadors menors. Els resultats obtinguts es contradiuen amb aquesta afirmació.

El temps de vida de la fotoluminescència és inversament proporcional al ràtio de l'emissió espontània. S'obté un temps de vida menor per al menor separador, però els temps de vida corresponents a la resta de separadors no segueixen el comportament esperat.

S'ha comprovat com l'augment de la fotoluminescència depèn del metall i de la distància entre l'emissor i el metall. S'han obtingut resultats millors per a mostres cobertes de plata que d'or. Això és degut a la major rugositat de la plata respecte l'or, que extreu més eficientment els polaritons plasmònics superficials. L'augment en la fotoluminescència també és degut a que la freqüència de plasma de la plata és major que la de l'or i doncs, la plata reflecteix més llum que l'or a la freqüència de treball.

L'augment de la fotoluminescència observat pot ser degut a l'existència de polaritons plasmònics superficials o degut a l'efecte de fina pel·lícula causat per la superfície del metall. S'hauria de continuar estudiant per arribar a conclusions més satisfactòries.

1 Introduction

Since the invention of the light bulb in 1879 by Thomas Edison there has been a lot of interest in being able to control the emission of light.

Although many years have passed since that moment, light emission is still a very actual subject. New kinds of light sources have appeared, for example Light Emitting Devices (LEDs) or lasers. New materials are being investigated in order to improve their efficiency and production cost. Spontaneous emission is found in LEDs or lasers, for example. We would like to enhance spontaneous emission in order to have more efficient devices that can emit more light than others or to reduce laser's threshold values. A possible way to enhance light emission is by the use of Surface Plasmon Polaritons (SPPs). This is a recent field and that is why not much literature is found talking about it. So in this thesis we are going to study the role of SPPs in the enhancement of light emission.

This thesis is arranged in the following way. First of all we are going to present Organic Light Emitting Devices (OLEDs), as it is one of the most important applications of light emission nowadays and a lot of advances are done to improve their efficiency. Then I will explain some theory in order to be able to understand the rest of the thesis. After that I will explain the experimental procedure that I have followed to work in the thesis and later the obtained results are presented.

1.1 Motivation: OLEDs

Spontaneous emission plays an important role in many devices like LEDs or Lasers. Basic research about manipulating the spontaneous emission can help to optimize the performance of these devices. Spontaneous emission manipulation can be separated in two categories: Spontaneous emission inhibition and enhancement. This two kinds of manipulations can be performed also in particular spatial direction. For example enhancing the spontaneous emission in a laser cavity in the direction of the cavity can lower the threshold, when then laser switches from spontaneous emission to stimulated emission. One of the most popular applications of spontaneous emission manipulation is the enhancement in LEDs. I the following I will discuss the

functionality and applications of a special LED, namely the OLED. I will start with a brief history.

During the last years research in organic materials and, particularly, Organic Light Emitting Devices (OLEDs), have been increasing a lot with the objective of improving the characteristics and longevity of OLEDs. OLEDs are called to be the substitutes of LCDs and inorganic LEDs. First of all I am going to explain how the interest in using organic materials began.

Electroluminescence is the light generation that is obtained when an electric field is applied to a material. It is caused by the recombination of electrons and holes in both organic and inorganic substrates with the existence of an external circuit. [1]

Electroluminescence was observed for the first time in inorganic materials in 1936. It was seen in a ZnS phosphor powder dispersed in an isolator and placed between two electrodes by Destriau et al. [2]. Later, at the beginning of 1960s, the first commercial Light Emitting Devices (LEDs) were built using the inorganic semiconductor GaAsP [3].

The energy of emitted photons, and so the color of the LED, are dependent on the semiconductor used to build the LED, particularly the energy gap of this material. That is the reason why at the beginning LEDs were not available in many colors. Then, as research went on, more color LEDs were built. Materials used in those LEDs came from elements of the III and IV groups of the periodic table, as for example GaAs, GaP, AlGaAs, InGaP, GaAsP, GaAsInP or AlInGaP.

Then, research was focused on finding more efficient materials and fabrication techniques improvement.

In organic materials electroluminescence was observed for the first time in 1963 for anthracene [4] [5]. But at that time efficiencies and lifetimes for inorganic materials were better than for organic materials. Therefore, research was focused on inorganic materials and organic materials were abandoned during a period.

Later, an important advance for organic materials was done in 1990, when Friend et al. discovered how to produce large area displays by simple coating techniques. This allowed cheaper and more efficient devices.

As mentioned above, at the beginning, inorganic LEDs research was more advanced than OLEDs, but nowadays organic technology has overcome the inorganic one. Among other things, it is very easy to get different colors with OLEDs, including white color. This fact makes organic technology very interesting.

Lately a lot of research has been done in this field, not only by universities, but also by companies interested in getting more market share. Some aspects that were interesting to improve were the devices efficiencies and lifetimes and the development of materials that may be used for new applications or getting new colors.

The functionality of an OLED is as following. When some voltage is applied at the electrodes of the OLED, a carriers flow is obtained. Holes at the anode and electrons at the cathode are introduced into the organic material and move to the opposite electrode. However, if a hole and an electron find each other in their way to the other side of the OLED, they build an exciton and this exciton recombines spontaneously while emitting a photon, according to the band gap of the material.

Researchers can estimate the efficiency of their devices in different ways.

Due to refraction, all photons emitted in the organic material cannot be seen by an external observer. We distinguish the internal quantum efficiency and the external quantum efficiency. The ratio between the number of emitted photons and injected electrons is called internal quantum efficiency. The extraction efficiency is the fraction of light which can escape from the device. Internal quantum efficiency is related to the measured external quantum efficiency by the following equation:

$$\eta_{\text{int}} = 2n^2 \eta_{ext} \qquad (1.1)$$

Where η_{int} and η_{ext} are the internal and external quantum efficiencies, respectively, and n is the refractive index of the organic layer.

We can also determine the power efficiency η_{pow} , the ratio between output light power and input electric power:

$$\eta_{pow} = \eta_{ext} E_p U^{-1} \qquad (1.2)$$

Where E_p is the average energy of emitted photons and U is the applied voltage.

Then we can calculate the luminous efficiency, η_{lum}, bearing in mind that the human eye has different sensitivity for each color, from the following expression:

$$\eta_{lum} = \eta_{pow} S \qquad (1.3)$$

Where S is the eye sensitivity curve, defined by the Comission Internationale de l'Eclairage (CIE).

Another important parameter of an OLED is its brightness (in cd m^{-2}) [6] [7].

The general structure of an OLED is the following:

- Substrate: it supports the OLED and it can be done of plastic or glass, for example.
- Anode: it removes electrons when a current is applied at the OLED.
- Organic layers: they are made of organic molecules or polymers.
    - Conducting layer: it transports holes from the anode.
    - Emissive layer: it is the part where light is done. It transports electrons from the cathode.
- Cathode: it transports electrons when a current is applied at the OLED.

Figure 1.1 shows the structure of a generic OLED:

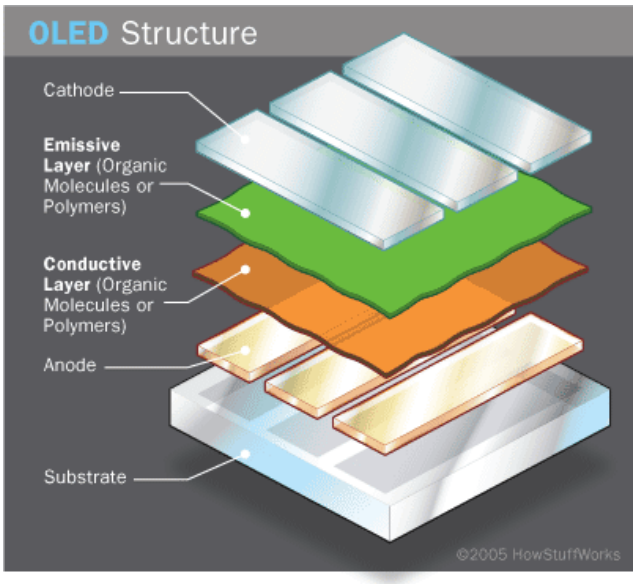

Figure 1.1: Structure of an OLED. [8]

With OLEDs, there is the possibility of producing large area and small thick displays. This can be useful for some applications in the future such as roll-up TV screens or some display monitor built into clothing. They are cheap to produce and they do not use much power. This is very interesting for portable applications. Their color and brightness can be modulated in a really simple way with some structural modifications.

Comparing OLEDs to LCD, OLEDs have faster refresh rate and better contrast and brightness. The screens are brighter and have a fuller viewing angle.

However, they have also some disadvantages, although they have more positive than negative aspects. One of the problems they have is their short lifetime when compared to TFTs (red and green OLED can last up to 200000 hours, while blue OLEDs only last 14000 hours, according to *http://OLED-info.com*). Nowadays companies are working to solve this problem. Another disadvantage is that they can be easily damaged by water.

We can find very interesting applications for OLEDs. Production of large flat area displays is useful for applications where space is limited, such as inside cars or airplanes. Flexible OLEDs have also an interesting application to build roll-up devices or displays on curved surfaces.

There are several ways to produce OLEDs. The great difference between them is the way how the organic layers are deposited onto the substrate. Then, they are going to be described:

- Vacuum deposition or vacuum thermal evaporation: in a vacuum chamber, organic materials are evaporated onto cooled substrates. This process is expensive and inefficient.
- Organic vapor phase evaporation: in a low pressure chamber, evaporated organic molecules are transported by a carrier gas and deposited onto cooled substrates. This process makes OLEDs production cheaper.
- Inkjet printing: OLEDs are printed onto substrates. This process makes OLEDs production much cheaper and allows the construction of large area displays.

There are many kinds of OLEDs, depending on the type of molecules they are made of. They can be separated in two main groups: small molecule OLEDs and polymer OLEDs.

Small organic molecules were used in the first OLEDs depositing them onto a substrate by vacuum deposition, an expensive and inefficient process.

Large polymer molecules OLEDs are cheaper and can be used to produce large area displays.

Light-emitting polymers have the major advantage that they are soluble and therefore can readily be deposited in solution onto a display substrate — for example, by spin-coating or ink-jet printing — without the need of a temperature-controlled vacuum-environment. P-OLED (polymer OLED) displays can have larger screen sizes that can be made than with small-molecule OLEDs as there is no need for the shadow masks required by the vacuum deposition processing of the latter. P-OLED displays arguably also operate at lower voltage and are more power-efficient than small-molecule ones [8]. In figure 1.2 an OLED classification is shown.

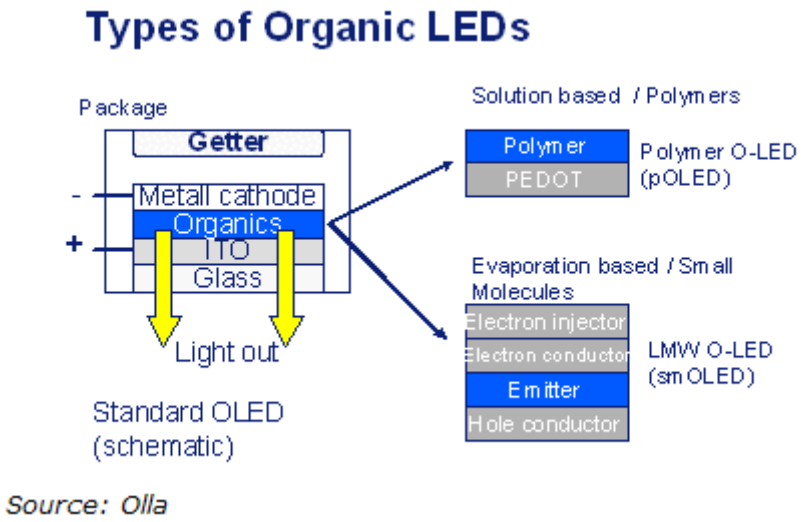

Figure 1.2: Types of Organic LEDs [9]

In the near future, it is expected that OLEDs reach all the market that actually belongs to usual LEDs and LCDs and some new applications such as:

- Signage
- Back lighting
- General illumination
- Specialty lighting
- Architecture lighting
- Automotive controls and instruments
- Consumer electronics
- Digital entertainment
- Digital photography and digital imaging
- Manufacturing systems engineering
- Medical equipment
- Micro displays
- Mobile communications
- PCs, notebooks
- Personal / Mobile storage and MP3 components
- Telecommunications
- Telematics and navigation

2 Theory

In this chapter the basic theory knowledge is going to be briefly explained in order to be able to understand in an easier way the following chapters.

Light emission of electronic devices such as LEDs or LASERs is based on Spontaneous Emission (SE). The objective of our work is the enhancement SE using Surface Plasmon Polaritons (SPPs).

So, the first point that is going to be treated is SE. Two kinds of SE can be found: phosphorescence and fluorescence. Both of them will be introduced, a deeper explanation will be given for fluorescence, because in our experiments we will use fluorescence to excite the SPPs. Then it is going to be explained the relationship existing between the SE rate and the Photoluminescence (PL) lifetime. After that, we are going to explain what are SPPs and their properties.

An excited SPP is captured to the metal dielectric interface, this will not contribute to useful light. Using the surface roughness of the metal dielectric interface we scatter out the SPP. Therefore fundamental knowledge about surface roughness is given.

2.1 Spontaneous Emission

2.1.1 Description

Spontaneous emission (SE) is the emission of a photon by an atom, accompanied by a transition of the atom from an electronic state of energy E_2 to one of lower energy E_1 [10]. The SE of a photon process is shown in figure 2.1. The photon will have a frequency v and an energy $E_2 - E_1 = hv$, where h is Planck's constant. In SE unlike to stimulated emission, the photon's phase and its propagation direction are random. Light produced by spontaneous emission is called luminescence.

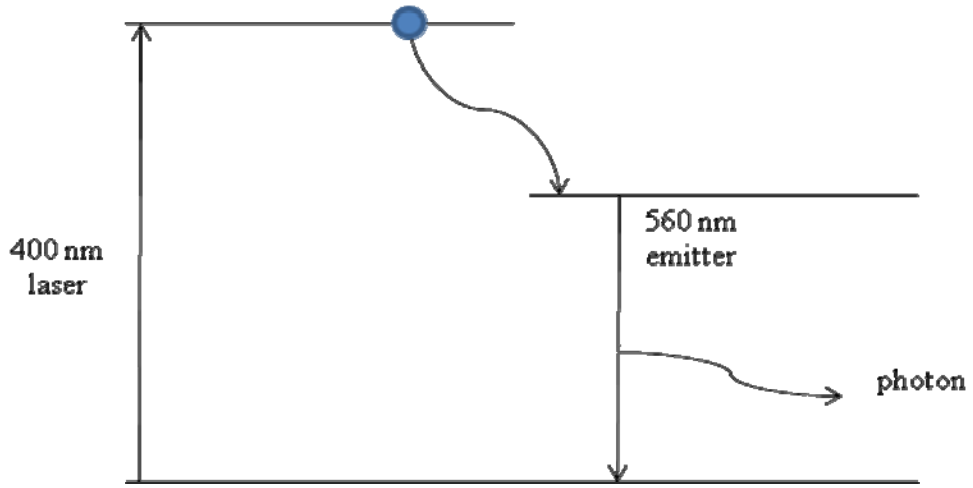

Figure 2.1: Spontaneous emission of a photon

Decay or relaxation can happen in two different ways: radiatively and no radiatively. In no radiative relaxation, energy is released as phonons or heat. Non radiative relaxation happens when the energy difference between levels is very small, and this usually occurs on a much faster time scale than radiative transitions. For many materials, such as semiconductors, electrons jump quickly from a high energy level to a metastable level, through non radiative transitions of very small energy difference and then they go down to the bottom level through a radiative transition (over the band gap in semiconductors).

There are two kinds of SE: fluorescence and phosphorescence.

Fluorescence is a luminescence phenomenon in which electron de-excitation occurs almost spontaneously, and in which emission from a luminescence substance ceases when the exciting source is removed.

Phosphorescence is similar to fluorescence, but the species is excited to a metastable state from which a transition to the initial state is forbidden. Emission occurs when thermal energy raises the electron to a state from which it can de-excite.

So, the biggest difference between fluorescence and phosphorescence is that fluorescence is faster than phosphorescence (usually fluorescence occurs in some nanoseconds, while phosphorescence in some milliseconds). It is also known that

fluorescence stops when the exciting source disappears, while phosphorescence can last after removing the excitation. Some daily objects where they can be found are the fluorescent lights (fluorescence) or the glow in the dark objects, like some watches (phosphorescence).

2.1.2 Fluorescence

Fluorescence is the phenomenon that occurs in some molecules called fluorescent dyes. The electronic-state diagram (Jablonski diagram) shown in figure 2.2 illustrates the fluorescence process:

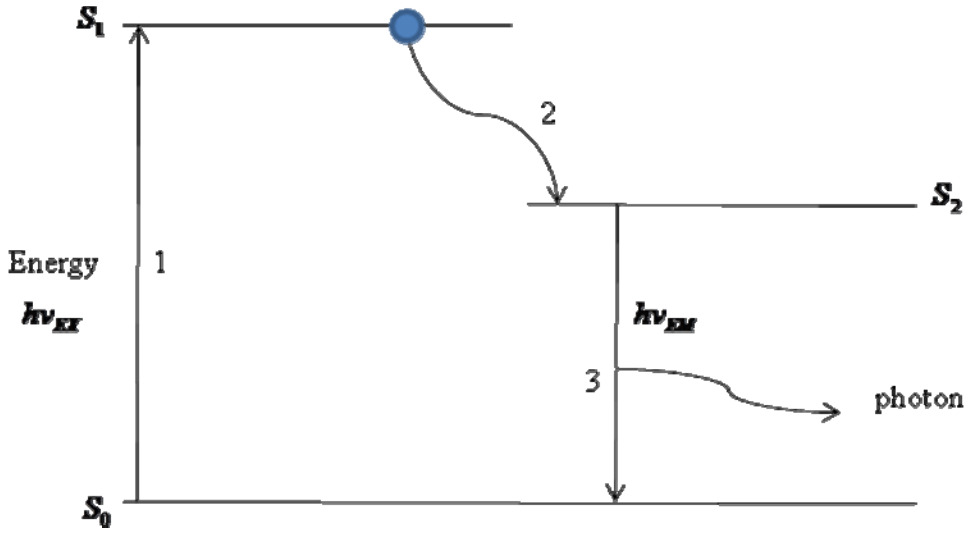

Figure 2.2: Fluorescence process

An excited electronic singlet state is created by optical absorption and fluorescence emission.

In state 1, a photon of energy $h\nu_{EX}$ is created by an external source such as a laser and afterwards an excited electronic singlet state appears. The excited state exists during a limited lifetime (usually beneath 10 ns). After this time part of the energy $S_1^{'}$ is dissipated yielding a relaxed singlet excited state S_1 from where emission occurs. However, not all the molecules in $S_1^{'}$ yield to the state S_1. Some of them are lost by other processes. The fluorescence quantum yield is the ratio between the number of

fluorescent photons emitted and the number of photons absorbed. In the last state, a photon of energy hv_{EM} is emitted returning the fluorophore to its initial energy.

The energy of the emitted photon is lower than the excitation photon's one. Therefore, the emitted photon wavelength is higher than the excitation photon's one. This difference of energy is called Stokes shift and it is determined by $(hv_{EX} - hv_{EM})$. This is an important fact that allows us to difference between the emitted energy and the absorbed one. It also avoids that some excitation is produced by the same fluorophore.

A way to determine the fluorescence intensity that a fluorophore can generate after an excitation of a specific wavelength can be known from the study of the emission spectra like the on e that is shown in figure 2.3. The emission spectra intensity is proportional to the amplitude of the fluorescence excitation spectrum at the excitation wavelength.

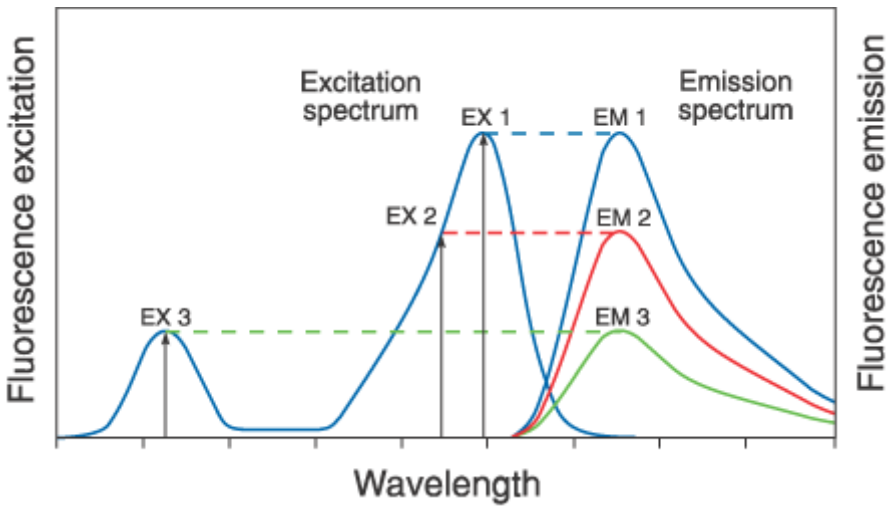

Figure 2.3: Fluorescence spectra [10]

Excitation of a fluorophore at three different wavelengths (EX1, EX2, EX3) does not change the emission profile but does produce variations in fluorescence emission intensity (EM1, EM2, EM3) that correspond to the amplitude of the excitation spectrum.

Apart from this dependence of the emitted intensity on the excitation wavelength, when a mixture of fluorophore with other elements is done, this intensity also depends on other parameters. These parameters are the molar extinction coefficient, optical path length and solute concentration. The emission spectra can also depend on the kind of solvent used.

Although, in general, the process of excitation and posterior fluorescence emission is cyclic, under high intensity illumination conditions the fluorophore can get damaged and then the fluorescence can get affected [10].

2.1.3 Spontaneous Emission rate and lifetime

Going back to spontaneous emission, some expressions are going to be studied.

When we have a numerous joint of N atoms on the highest state, the rate at which N decays is:

$$\frac{\partial N}{\partial t} = -A_{rad} N \qquad (2.1)$$

Where A_{rad} is the rate of spontaneous emission (A Einstein coefficient). The above equation can be solved as:

$$N(t) = N(0) e^{-A_{rad} t} \qquad (2.2)$$

Where $N(0)$ is the initial number of atoms in the excited state and A_{rad} is the radiative decay rate of the transmission. The number of excited states N thus decays exponentially with time, similar to radioactive decay. The radiative decay rate A_{rad} is inversely proportional to the lifetime τ_{rad}:

$$A_{rad} = \frac{1}{\tau_{rad}} \qquad (2.3)$$

The rate of spontaneous emission is described by Fermi's golden rule. In a homogeneous medium, it is given by the following equation [11]:

$$A_{rad}(\omega) = \frac{\omega^3 n |\mu_{12}|^2}{3\pi\varepsilon_0 \hbar c_0^3} \qquad (2.4)$$

Where ω is the emission frequency, n is the refraction index, μ_{12} is the transition dipole moment, ε_0 is the vacuum permittivity, $\hbar$ is Dirac's constant and c_0 is the vacuum light speed.

To manipulate SE it is important to control the quantity of optical modes and their spatial distribution relative to the emitter [12]. The way in which SPPs help in the enhancement of SE is explained by Purcell effect.

Purcell effect was discovered when it was seen that there was an enhancement on SE rates of atoms when they were matched in a resonant cavity. With photonic materials the rate of radiative recombination of an embedded light source can be controlled [13]. If there is an enhancement in SE due to SPPs a reduction in the lifetime is also observed.

2.2 Surface Plasmon Polaritons

Surface Plasmon Polaritons (SPPs) are electromagnetic modes constituted by a light field coupled to a collective electron oscillation propagating along an interface between a metal and a dielectric. As SPPs are surface waves, their field intensity has its maximum on the interface and decays exponentially along the directions perpendicular to it [14]. It is said that the field in this perpendicular direction is evanescent as a consequence of non radiative nature of SPPs, which does not allow power propagation out of the surface.

One of the most interesting properties of SPPs is their capacity to concentrate and guide the light in sub wavelength structures. This could lead to circuits with smaller dimensions than actual ones. In these circuits, we would transform the light in SPP, then propagate and process it with some optical elements and turn it to light again.

We can also control SPPs properties in order to use them for specific applications such as optics, magneto-optics data storage, microscopy, solar cells or sensors [15].

When emitters placed near a metal decay via SE they may do it in three different ways. They may produce useful radiation, they may produce SPPs and they may be lost to absorption in the metal. SPPs are non radiative and thus, can not be seen. Between SPPs and visible light there is a momentum mismatch. If SPPs are coupled to light using some techniques that are going to be explained later, they may be added to directly emitted light and thus enhance SE. Some experimental results show that SPP's emission is much stronger than directly emitted light [16]. Concretely in OLEDs, the close proximity of the excitons to the metallic cathode used to inject electrons means that much of the power that would otherwise have been radiated is in fact lost to SPP modes on the cathode surface, thus detracting from device's efficiency[17-20].

Managing and, if necessary, recovering this power through the use of a periodic nanostructure or a rough surface is likely to be important for many future device designs, especially for high-efficiency, long life and full-color devices. The inverse process, that consisting in the use of SPPs to enhance the absorption of light, for example, in solar cells, is also of interest [15].

Going out from Maxwell's equations:

$$\nabla \times \vec{E} = -(1/c)\partial_t \vec{H} \qquad (2.5)$$

$$\nabla \times \vec{H} = (4\pi/c)\vec{j} + (1/c)\vec{E} \qquad (2.6)$$

Combining the equations, we get the wavelength equation at the metal. In frequency domain:

$$\nabla^2 \vec{E}(\omega) = \frac{\omega^2}{c^2}\left(1 + i\frac{4\pi\sigma(\omega)}{\omega}\right)\vec{E}(\omega) = \frac{\omega^2}{c^2}\varepsilon_m(\omega)\vec{E}(\omega) \qquad (2.7)$$

The dielectric constant of the metal is:

$$\varepsilon_{metal}(\omega) = 1 + i\frac{4\pi\sigma(\omega)}{\omega} = 1 + i\frac{4\pi}{\omega}\left(\frac{ne^2\tau/m^*}{1 - i\omega\tau}\right) = 1 - \frac{\omega_p^2}{\omega(\omega - i/\tau)} \qquad (2.8)$$

If the dielectric constant behavior with the frequency is studied:

$$\varepsilon_{metal}(\omega) = 1 - \frac{\omega_p^2}{\omega(\omega - i/\tau)} \underset{\omega\tau<<1}{\approx} 1 - \frac{\omega_p^2}{\omega^2} \qquad (2.9)$$

$\omega > \omega_p \rightarrow \varepsilon_m(\omega) > 0$ Propagating solution of wavelength equation

$\omega < \omega_p \rightarrow \varepsilon_m(\omega) < 0$ Evanescent solution of wavelength equation

$\omega = \omega_p \rightarrow \varepsilon_m(\omega) = 0$ Surface Plasmon Polariton

The result is shown in figure 2.4.

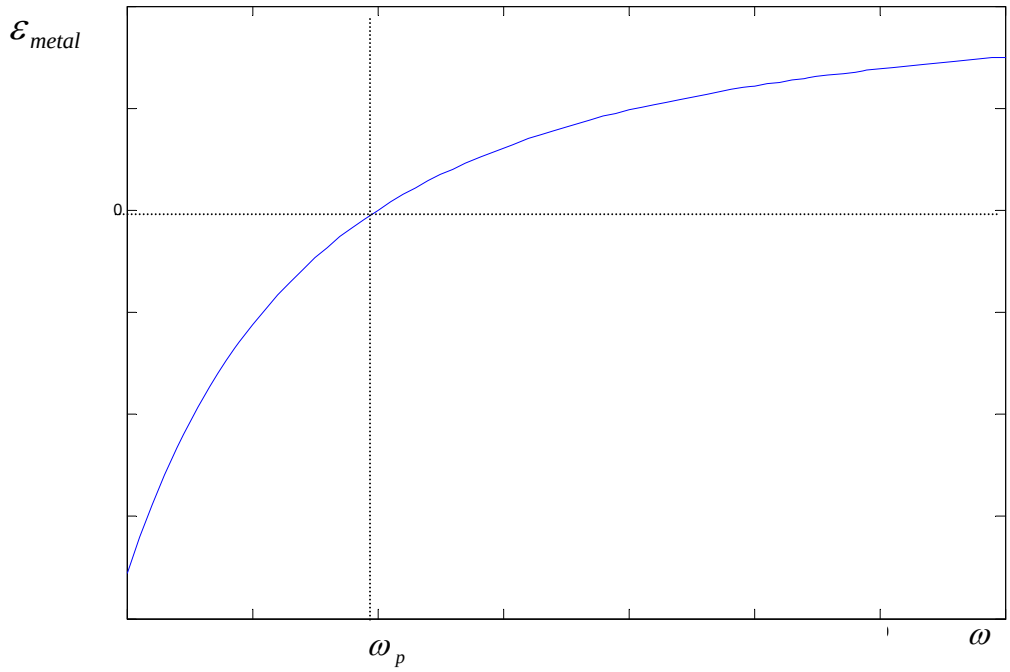

Figure 2.4: Dielectric constant of the metal. SPPs are found at the point where the dielectric constant equals to 0.

Our SPPs are different depending on the different relative permittivities, ε , of both metal and dielectric material. Solving Maxwell's equations with the appropriate boundary conditions, we get the wave vector of the SPP, k_{SP} :

$$k_{SP} = k_0 \sqrt{\frac{\varepsilon_d \varepsilon_m}{\varepsilon_d + \varepsilon_m}} \qquad (2.10)$$

Where ε_d and ε_m are the relative permittivities of dielectric and metal, respectively; and $k_0 = \omega/c$ is the free space wave vector.

ε_d and ε_m must have opposite signs if SPPs are to be possible at such an interface. This condition is satisfied for metals because ε_m is both negative and complex.

SPPs at the interface between a metal and a dielectric have a mixture between an electromagnetic wave and surface charge behavior. We have a magnetic field parallel to the surface and an electric field normal to it, in order to generate surface charge. The electric field normal to the surface has its maximum on the same surface and then decays with the distance following an exponential equation. It can be seen in figure 2.5.

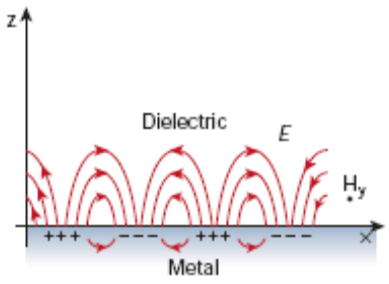

Figure 2.5: Electromagnetic field due to SPPs [15].

In figure 2.6 the evanescent behavior of the electric field can be seen. This way power is prevented from escaping out of the surface. In the dielectric material, the decay length of the field, δ_d, is of the order of half the wavelength of the light involved, while in the metal, δ_m is determined by the skin depth.

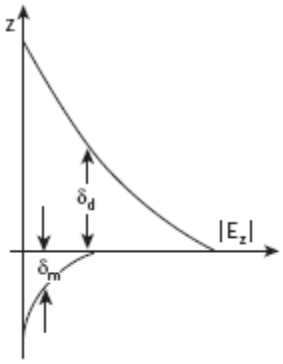

Figure 2.6: Decay length of the field (δ_d) and decay length into the metal (δ_m) [15].

In the dispersion curve of a SPP, we can see that there is a momentum difference between light and the SPP, which may be a problem to couple them together. The SPP has always a greater momentum, $\hbar k_{SP}$, than a free space photon, $\hbar k_0$ for the same frequency. It can be observed in figure 2.7.

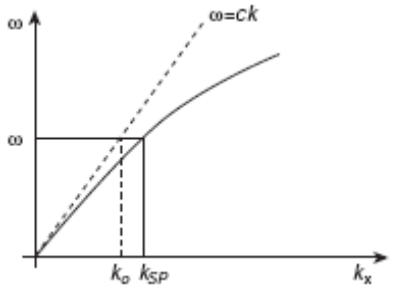

Figure 2.7: SPPs dispersion curve [15].

As k_x grows up, the density of plasmon modes is higher, tending to a flat line, and corresponding to a high field enhancement. Light that is incident over a wide range of angles can excite these modes. Flat bands are also associated with the localized SPP modes of metallic nanoparticles [21-22]. The frequency and width of these modes are determined by the particle's shape, material, size and environment [21] [23-24].

Once light has been coupled to SPPs, it is difficult to scatter it out without any additional element. In order to scatter out light several techniques may be used such as

prism coupling, the use of a periodic corrugation or grating in the metal's surface and, in our case, the use of a rough surface.

2.3 Roughness

As it has been mentioned before, a SPP is an oscillating surface charge density coupled to an electromagnetic field at the interface between a metal and a dielectric. Sometimes we are interested in controlling the SE rate of a surface. The momentum of a SPP is higher than the momentum of the light at the same frequency. That is why different elements are needed to be able to scatter out light of SPPs. We can do it using a grating, prism or making use of the characteristic roughness of the material. In our case, the use of the material roughness will be studied.

Roughness is a surface characteristic. It is defined by the vertical deviations of the ideal form of the surface. The higher these deviations are the rougher a surface is. Roughness determines many of the surface properties such as friction coefficients. For some applications, as the coupling of SPP to light, we are interested in controlling that surface.

The roughness of a surface can be measured in different ways: contact methods (dragging a measurement stylus across the surface) or non contact methods such as interferometry, confocal microscopy, electrical capacitance or electron microscopy.

In the trace of the roughness profile there are n ordered, equally spaced points. y_i is the vertical distance between a data point and the average height. The wavelength of the lowest frequency filter that will be used to analyze the data is usually defined as the sampling length.

The roughness of a surface can be characterized by some parameters. The most important parameters are the arithmetic average of absolute values (R_a), the root mean squared (R_{RMS}) and the maximum height of the profile (R_t). They are defined by the following equations:

$$R_a = \frac{1}{n}\sum_{i=1}^{n}|y_i| \qquad (2.11)$$

$$R_{RMS} = \sqrt{\frac{1}{n}\sum_{i=1}^{n} y_i^2} \qquad (2.12)$$

$$R_t = R_p - R_v \qquad (2.13)$$

Where R_p and R_v are the maximum peak height and the maximum valley depth, respectively.

These parameters are going to be calculated for gold and silver, metals used in our experiment, in chapter 3.

2.3.1 Mie theory

Mie theory is a rigorous solution for the scattering intensity by an isotropic sphere embedded in a homogeneous medium.

The usual optics phenomenon like light refraction or reflection in the macroscopic world have a different behaviour when the particle's sizes are smaller or comparable to the wavelength of the light [25-26].

Mie theory defines two kinds of scattering depending on the relation between the particle size and the wavelength of light. We talk that we have Rayleigh scattering when the particles size is up to about ten times smaller than the wavelength of the light or Mie scattering when the particles size is comparable to the wavelength of light.

Rayleigh scattering intensity is strongly dependant with the wavelength of light (λ), following the equation:

$$I \propto \left(\frac{a}{\lambda}\right)^4 \qquad (2.14)$$

Where a is the radius of the scattering particle. Thus, Rayleigh scattering intensity is stronger for short wavelengths of light.

For bigger particles, we have to talk about Mie scattering. Mie scattering is not strongly dependant on the wavelength and its pattern is like an antenna lobe, with a sharper and more intense lobe for larger particles [27].

But how can Mie theory explain the scattering for a rough surface?

It has been demonstrated in reference 28 that for small heights of the roughness profile, the scattering is bigger at shorter wavelengths, as happens in Rayleigh scattering. But as the roughness profile increases, the scattering tends to a maximum, as happens with Mie scattering.

The explanation of this is that the surface roughness can be modelled like if it was formed by small spheres with diameter the height of the profile. So, the light scattering properties of a surface are dependent on its roughness profile.

3 Technology

It is wanted to investigate the enhancement in photoluminescence that can be reached by joining a metallic surface with an emitter using a spacer between them, as it is showed in figure 3.1.

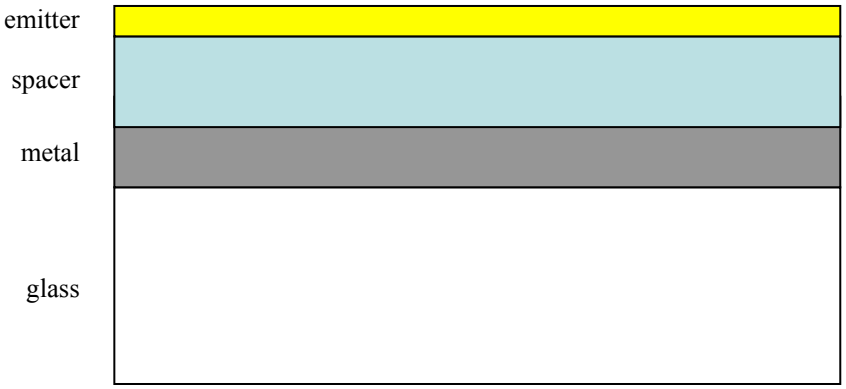

Figure 3.1. Geometry of the sample

The effect that different kinds of metal coatings have with different spacer thicknesses is going to be studied.

The chosen metals are gold (Au) and silver (Ag). Different kinds of spacers will be also tried: tantal pentoxide (Ta_2O_5) and polymethylmethacrylat (PMMA) with thicknesses going from 10 to 150 nm. The different kinds of samples that are wanted to be produced are shown in the following diagram:

METAL / SPACER	Ag	Au
10nm	Emitter 515nm Emitter 560nm Emitter 605nm	Emitter 515nm Emitter 560nm Emitter 605nm
50nm	Emitter 515nm Emitter 560nm Emitter 605nm	Emitter 515nm Emitter 560nm Emitter 605nm
100nm	Emitter 515nm Emitter 560nm Emitter 605nm	Emitter 515nm Emitter 560nm Emitter 605nm

From now on, the process that has been followed to produce the samples is explained.

3.1 Substrate (clean room)

Substrates are glass (float glass) squares of 16 mm long side and 1 mm thick cleaned in the following way: first of all ultrasonic cleaning is applied during ten minutes with acetone, ten minutes with isopropanol and then with deionised water at the highest voltage. Besides ultrasonic cleaning, plasma cleaning has been done to remove impurities from the glass surface and enhance performances of our experiment.

It has been used a Diener Electronic Plasma-Surface-Technology device. This machine is used for surface cleaning, among other applications. Plasma is an ionized gas (neutral gas atoms are split into ions and electrons). In surface cleaning an ion bombardment cleanses physically the sample and, depending on the gas used, also

chemically. The contamination is vaporized and sucked away, as can be seen in the following pictures:

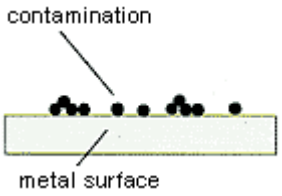

Figure 3.2: Metal surface with contaminations before plasma cleaning [29]

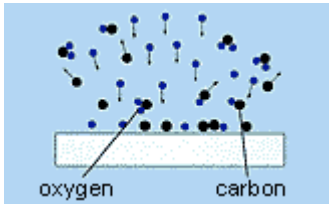

Figure 3.3: Carry off the contamination [29]

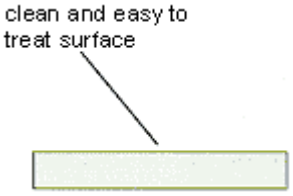

Figure 3.4: After the plasma cleaning without any contamination [29]

In our case, plasma cleaning has been done during 2 minutes using as gas O_2 and a pressure of 0.4 mbar, letting the samples ready for posterior treatments.

3.2 Metal

The discovery of surface Plasmon-coupled emission proved that nanometre sized metallic thin films (30–50 nm thickness) when located in the near field (100-200 nm) of

a LED or OLED emitting source, could substantially enhance the quantum yield and the radiation output of such a device [30-31].

In our experiment fifty nanometres of silver and gold were thermally evaporated on separate glass slides using an electron beam evaporating technique (UNIVEX) under ultra high vacuum, providing a continuous metallic film. A test sample for every metal was prepared by covering a part of the sample with a piece of glass, so that the metal is only evaporated in a part of the sample. In that way it is easier to measure the final thickness with DEKTAK8000.

First of all the metallic accessories have to be placed into the machine because UNIVEX needs different pieces depending if it has to work with metal or dielectric materials. The crucibles for the chosen materials have to be also placed, in this case gold and silver crucibles. Then the correct quartz crystal (for metallic depositions) has also to be placed. The quartz crystal's function is measuring the mass added to the face of the sensor and then the instrument's knowledge of the material's density (specified by the film's density parameter) allows conversion of the mass information into thickness. The correct parameters have to be configured. Z-ratio is a parameter that corrects the frequency change to thickness transfer function for the effect of acoustic impedance mismatch between the crystal and the coated material. Because of the flow of material from a deposition source is not uniform everywhere, it is necessary to account for the different amount of material flow onto the sensor compared to the substrates. This factor is controlled by the film's tooling parameter.

The parameters used for silver are 10.49 for density and 0.5 for Z-ratio. The parameters used for gold are 19.3 for density and 0.318 for Z-ratio. For both silver and gold a film's tooling parameter of 72 has been used.

Then when the machine begins its operation process, the vacuum is made during a minimum time of 2 hours. After that time a pressure of $8.5 \cdot 10^{-6}$ is reached. Then the Telemark's voltage is turned on and the filament current is also turned up. The beam is placed on the centre of the crucible. Then emission power is slowly increased until an optimal and constant rate is get. Final values of 7.04 kV and 31 mA for silver and 7.35 kV and 46 mA for gold are got. Deposition ratios of 1.2 Å/s for silver and 1 Å/s for gold are reached. After that, the shutter is opened and the metal deposition begins. After

the required thickness level is reached, the shutter is closed and the emission is reduced to zero again.

The real thicknesses of these layers were measured using a profilometer which has a resolution of 5 nanometres (DEKTAK8000, Veeco Metrology Group). With this machine we can examine briefly the surface and measure the thickness of the metal layer while a needle runs along the surface between the coated and the uncoated parts of the sample. For our experiment a stylus force of 10 mg and a scanning time of 60 seconds have been used. Surface variations make the stylus to be translated vertically and then converted to digital format. After that the surface profile is represented as a two dimensional profile which is plotted, scaled, and displayed on the video monitor. Thicknesses of 56 and 49 nanometres for gold and silver layers, respectively, are obtained.

Then the surface morphology of the sample was characterized by an Atom Force Microscope (AFM) Nano Wizard II (JPK Instruments, Berlin, Germany) using intermittent contact mode silicon cantilevers NCH-20 from NanoWorld. In this mode the cantilever does not run over the surface continuously, but going up and down at certain frequency.

The height image of the samples is shown in figure 3.5:

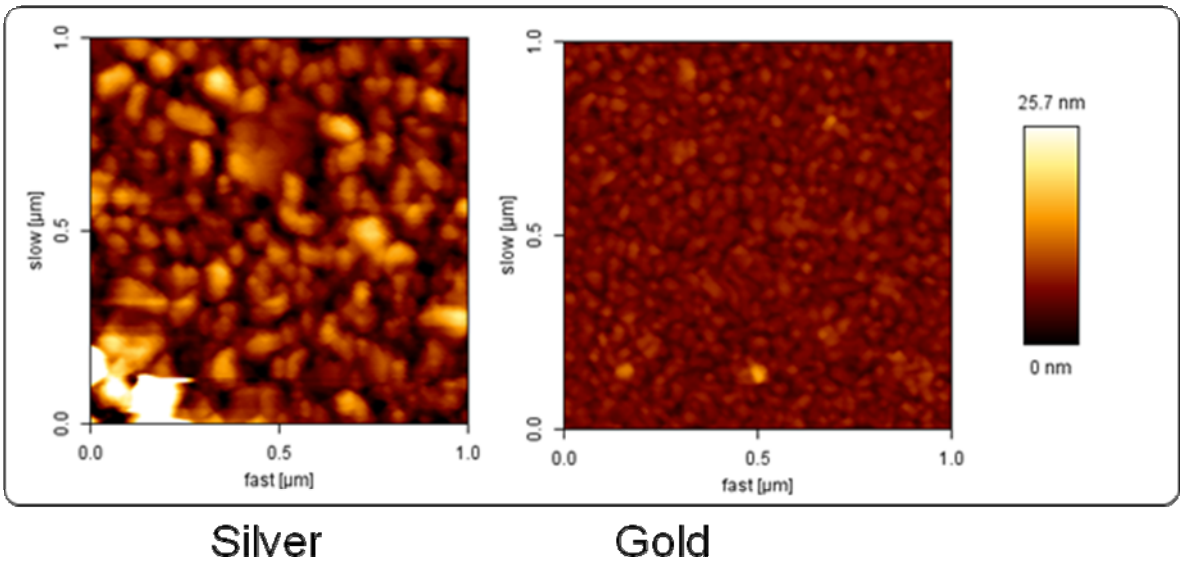

Figure 3.5. AFM contour height of the samples

The arithmetic average of absolute values (R_a), the root mean squared, (R_{RMS}) and the maximum height of the profile (R_t), that were already introduced in chapter 2 are going to be obtained for both gold and silver, and thus, have some reliable data to compare both surfaces. As an alternative to calculation using the equations given in last chapter, we are going to get them by making use of the utilities found in *JPK Image Processing*, software provided by the AFM manufacturer.

In the following table we can see the most important roughness parameters for gold and silver:

Parameter	**Gold**	**Silver**
R_t	6.396 nm	32.55 nm
R_a	1.014 nm	6.156 nm
R_{RMS}	1.247 nm	7.230 nm

Some results obtained by others [32] indicate that surface roughness plays a role in waveguide mode suppression. If the metal surface was perfectly flat, it would be difficult to extract light emission from the SPP, since it is a non propagating evanescent wave. However, roughness and imperfections in evaporated metal can scatter SPPs as light.

Analyzing the data in the table and the images of the samples, one can deduce that silver is rougher than gold and, thus, has to be better to scatter out light in our experiment. The maximum height of our profile is smaller than the excitation wavelength (emitted by the fluorospheres), and so it is Rayleigh scattering. As it was mentioned in the previous chapter, the scattering is higher for bigger particles and short wavelengths.

An important propriety of metals is their plasma frequency. Light of frequency below the plasma frequency will be reflected because the electrons of the metal screen

the electric field of the light. Light of frequency above the plasma frequency will be transmitted, because the electrons cannot response faster enough to screen it.

The Plasmon energy is defined by the following equation:

$$E_p = \hbar\sqrt{\frac{ne^2}{m\varepsilon_0}} \qquad (3.1)$$

Where n is the conduction electron density, e is the elementary charge, m is the electron mass and ε_0 the permittivity of the vacuum.

The surface Plasmon resonances are found at 650 nm and 558 nm for Au and Ag, respectively [33].

3.3 Spacer

Using spacer layers avoids several problems. It avoids chemical reactions between the polymer and the metal that can alter the emission characteristics of the polymer. It also rules out diffusion of the exciton to the metal as a necessary precondition for quenching. Furthermore, no diffusion of metal atoms into the polymer layer occurs. In addition, a comparison of the PL of a polymer film at various distances to the metal allows us to draw conclusions about the nature of the emission phenomenon.

Since the SPPs have their electric field confined to the metal surface, the separation of the emitters and metal has to be small, in order to have a good coupling of emitted light to SPPs. So, higher spontaneous emission enhancements are expected for thinner spacer layers.

3.3.1 PMMA

Polymethyl methacrylate (PMMA) is a polymeric material that can be used as a high resolution positive resist for direct write e-beam, x-ray and deep UV microlithographic processes or as a protective coating for wafer thinning, as a bonding adhesive and as a sacrificial layer. It can be exposed with various parts of the electromagnetic spectrum and, thus, PMMA is one of our candidates to be placed as spacer layer.

Before covering the metal surfaces with PMMA, some experiments over simple glass are done, to avoid possible damages to the metal surface.

The glass used as substrate is cleaned as explained before. Thicknesses between 10 nm and 120 nm are going to be tried and the chosen PMMA is AR-P 679.02, from Allresist, with a molecular-weight of 959K and a solids content of 2%. They are deposited onto the glass substrate by spin-coating. Spin-coater parameters are an initial speed of 500 rpm with a 5 seconds ramp and a speed maintenance of 5 seconds, and another 5 seconds ramp to get the chosen final speed during 35 seconds. After that the samples are placed on the hot plate at 150°C during 3 minutes. The optimal speeds are given by the manufacturer. It is wanted to get the relationship that exists between the spin-coating speed and the thickness of the layer. For that, different speeds of spin-coating have been tried. The chosen speeds have been 2000, 4000, 6000, 8000 and 10000 rpm. Then they have been measured with DEKTAK8000. The way in which the film thickness is measured is by scratching the sample surface with some tweezers (soft enough to not scratch the glass substrate). The PMMA layers were not homogenous and, because of that, several measurements were done and then averaged.

However, the thinnest layer that was obtained was 78 nm at 8000 rpm and thinner layers are needed for this experiment.

That is why the same product AR-P 679.02 is going to be soluted with acetic acid in order to reduce its solids content to 0.5%. This solution is prepared by the mixture of 2.5 ml of AR-P 679.02 and 7.5 ml of acetic acid. In this way, thinner layers are expected to be obtained. The thinnest layer obtained is 62 nm at 10000 rpm.

So, another solution of PMMA with a solids content of 0.4% is prepared. It is done by mixing 2 ml of AR-P 679.02 and 8 ml of acetic acid. Results shown in figure 3.6 have been obtained:

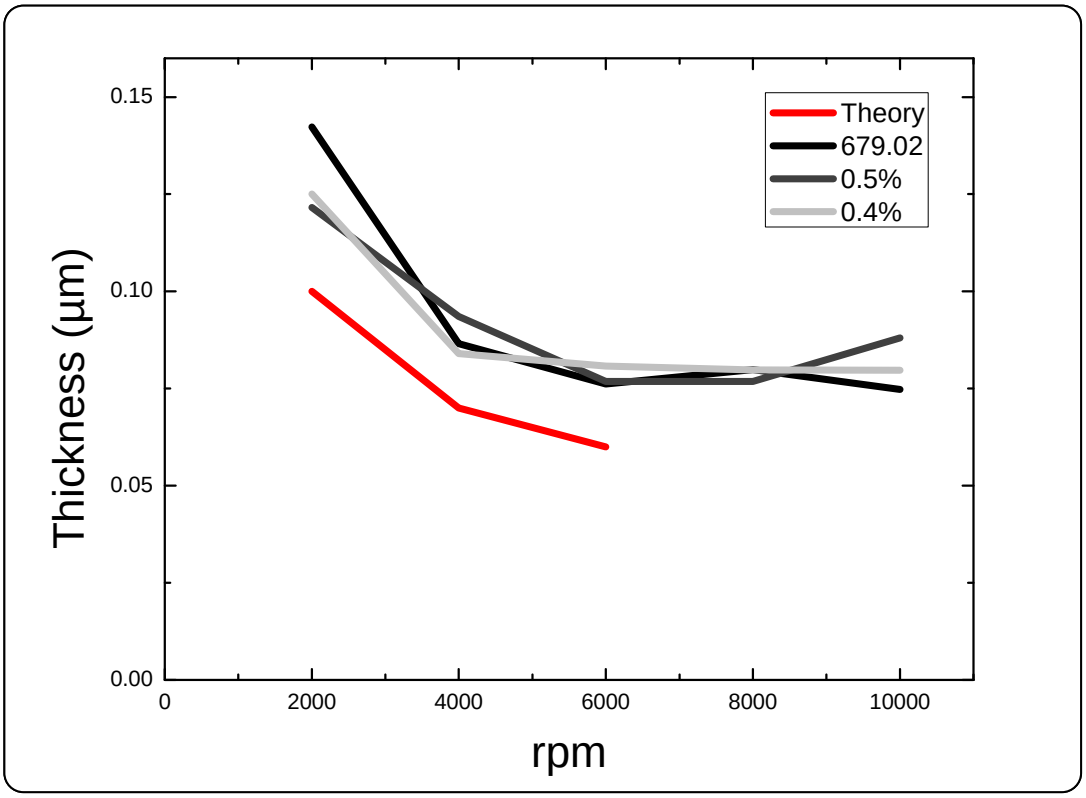

Figure 3.6. Relationship between the spin-coating speed and the PMMA thickness

So, the obtained results differ from the theoretical ones and it is found that small thicknesses are very difficult to reach. Thus, the use of PMMA as spacer is discarded.

3.3.2 Ta_2O_5

Tantal pentoxide (Ta_2O_5) is a high-index, low absorption material usable for coatings from 350 nm to around 8 µm regions. It has been chosen by its ease to work with. Its layers can be deposited by electron-beam evaporation or sputtering.

On the set of samples, Ta_2O_5 spacer layers of different thicknesses between 10 nm and 100 nm were evaporated on top of the metal film coated substrates using an electron-beam evaporation technique (UNIVEX), as it was proceed for the metal layers. Test samples were also produced for each thickness.

Contrary to the metal deposition, the dielectric accessories have been placed in the machine, as well as the correct oscillator and crucible. The parameters used for this operation are 8.2 for density and 0.3 for Z-ratio.

Then the vacuum process is begun and after a few hours a pressure of $8 \cdot 10^{-6}$ is reached. The following steps are the same as those done for the metal evaporation. Final values of 7.51 kV, 71 mA and a ratio of 1.2 Å/s have been got. After that the shutter is opened and closed when the desired thicknesses are reached. Thicknesses of 10, 50 and 100 nm were tried. Then the real thickness of these Ta_2O_5 layers was measured with DEKTAK8000 and found out that 15, 85 and 120 nm spacer layers were obtained.

3.4 Emitter

First of all it is wanted to compare the photoluminescence behaviour of different kind of emitters with gold and silver and the different spacer thicknesses prepared. The used emitters are FluoSpheres® Fluorescent Microspheres, provided by Molecular Probes, which have their maximum absorption/emission frequencies at 505/515, 540/560 and 580/605 nm and a diameter of 40 nm. The microspheres are stable for at least one year, provided recommended storage conditions are strictly observed. They need to be at about 4°C, avoiding freezing and protected from light.

Microsphere particles, which are hydrophobic by nature, will always tend to agglomerate. In aqueous suspensions, the only thing preventing this is the surface charge on the particles. Conditions that can lead to agglomeration include: 1) high concentration of particles; 2) high electrolyte concentration; and 3) neutralization of surface charge groups. To minimize these adverse conditions, it is always wise to keep the microsphere suspensions dilute. If agglomeration does occur, the particles can frequently be rescued by either diluting the microsphere suspension, adjusting the pH or reducing the ionic strength and then redispersing the suspension by means of a bath sonicator. In the case of very small particles (less than 0.1µm), the sonicated suspension can be briefly centrifuged at high speed (12000 rpm) to further remove agglomerates from the suspension (the monodisperse particles will remain in suspension under these conditions). If the particles do not redisperse with these treatments, the manufacturer

recommends trying a lower concentration of particles and reagents (beginning with a 50% reduction in concentration).

The emitter is prepared by mixing and strirring fluorospheres and deionised water and playing with their proportions in the mixture. First of all a solution concentration of 20 µl of fluorospheres with 4000 µl of water was done. After cleaning the metal samples by introducing them during 10 seconds in the plasma cleaning, the emitter is deposited on the surface by spin-coating one drop of this emitter. The spin-coater parameters are a 9 seconds ramp and an initial speed of 1000 rpm during 30 seconds, and then a 9 seconds ramp and a final speed of 2000 rpm during 30 seconds.

Then observation of the surface has been done with a microscope (Nikon eclipse TE2000-U) and it has been seen that there is a very low concentration of fluorospheres on the samples.

So, new solutions of 40:4000 (40 µm fluorospheres and 4000 µm of water) and 60:4000 (60 µm fluorospheres and 4000 µm of water) have been prepared. However, when these samples are watched on the microscope, it is seen that they have a very irregular profile and there are agglomerations of fluorospheres in some places.

To avoid that problem the pots containing the emitters have been put during one minute at highest voltage in the sonicator bath. After that, new spin coatings have been done with the 60:4000 solution and then good homogenous results have been obtained.

In picture 3.7 we can see the absorption and emission spectra for the chosen emitters while excited with a 405 nm laser. The figure has been taken from the manufacturer application *Fluorescence Spectra Viewer*, available from its web page, http://www.invitrogen.com.

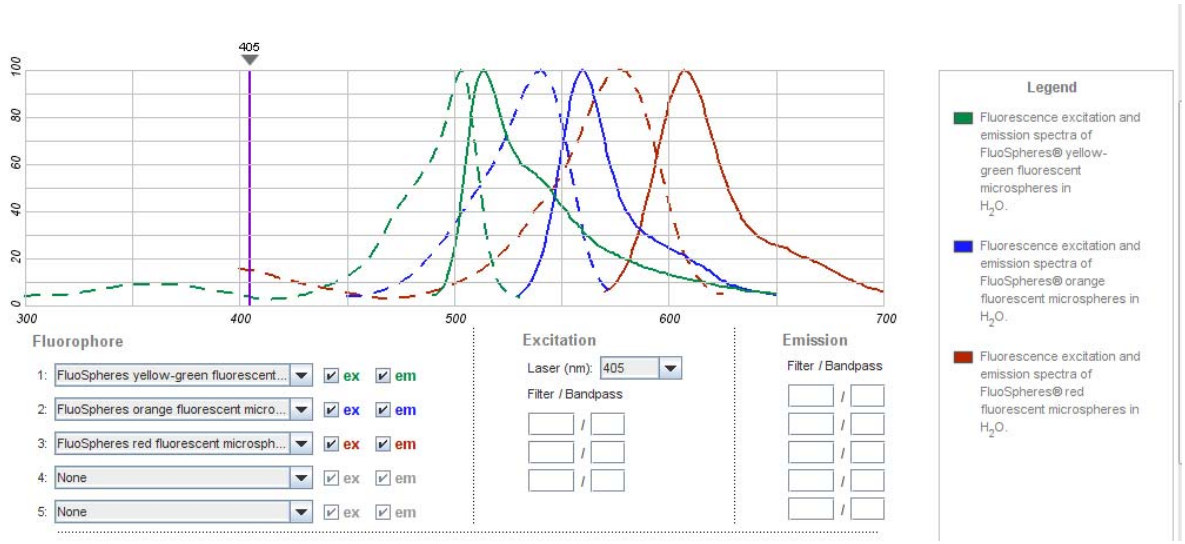

Figure 3.7: Fluorosphere's absorption-emission spectra

Once the production process of the samples is finished, the next step to follow is their characterization.

4 Measurements

The influence of gold and silver films on the light emission of the samples was compared. It was measured the photoluminescence of the gold and silver samples with different spacer thicknesses and compared with uncoated samples, so that the effect of the metal and the spacer layer in the photoluminescence enhancement could be studied.

Two different kinds of measurements were done to characterize the PL spectra of the samples.

Then, some measurements of the PL lifetime have also been done and explained later.

4.1 Photoluminescence intensity[1]

The method for PL measurements was the following and is illustrated in figure 4.1. The sample was mounted on a holder, excited from the top side part of the sample by a 400 nm frequency doubled mode locked Ti:Sa laser from an angle of 45° and its emission (also from the top side) collected by an optical fiber. Then the spectrum was analyzed by a monochromator and a Charge Coupled Device (CCD).

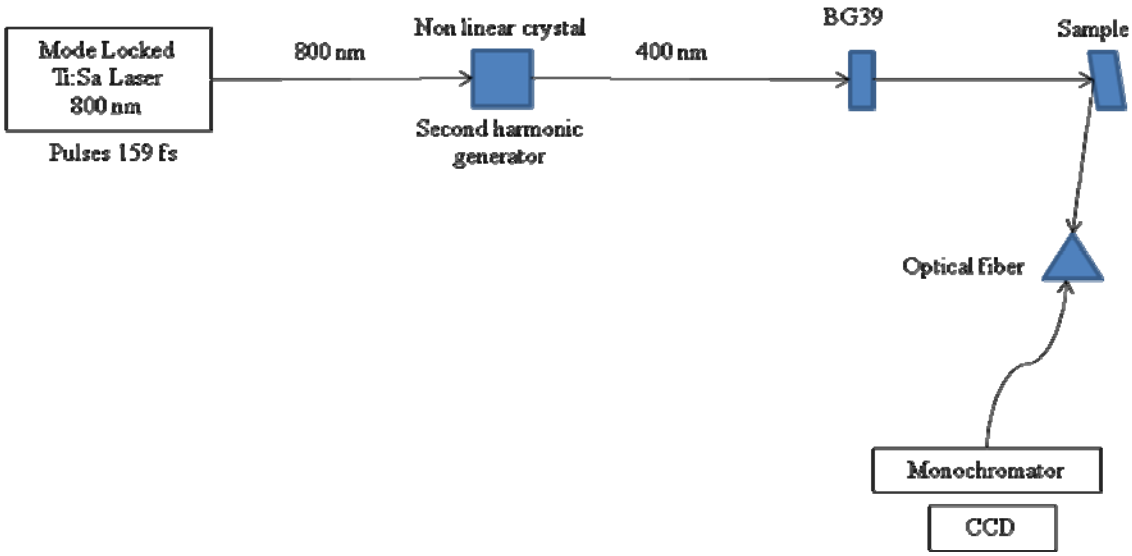

Figure 4.1. Photoluminescence measurement setup

[1] Matlab used files can be found in the appendix.

Transparent non linear crystals, can exhibit different kinds of optical nonlinearities which are associated with a nonlinear polarization. Nonlinear optic crystals are used for harmonic generation such as frequency doubling, frequency tripling or frequency mixing [34-35]. In our setup we use a LBO crystal for the second harmonic generation, we double the frequency of the laser to 400nm.

The function of BG39 filter is the elimination of the 800 nm light left from the second harmonic generation process. In picture 4.2 it can be seen the transmission spectra of BG39, with a transmission of $2 \cdot 10^{-5}$ at 8000 nm and 0.789 at 4000 nm.

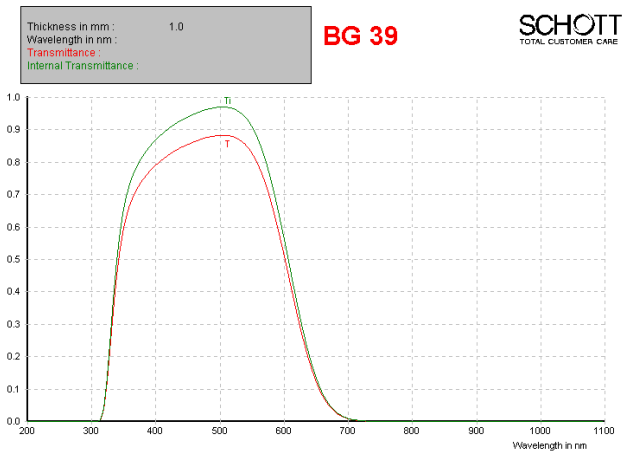

Figure 4.2. Transmission spectra of BG39 [36]

With the laser light, the fluorospheres were excited and thus, light was emitted and a fraction of it coupled to SPP's. The SPP is captured by the metal dielectric interface. However the surface roughness of the metal scatter out the SPP.

In picture 4.3 we can see the PL measurements for samples coated with silver and an emitter of 560 nm. Three different spacer thicknesses are shown: 10nm, 45, and 100 nm. These spectra were normalized to the PL of the sample without metal.

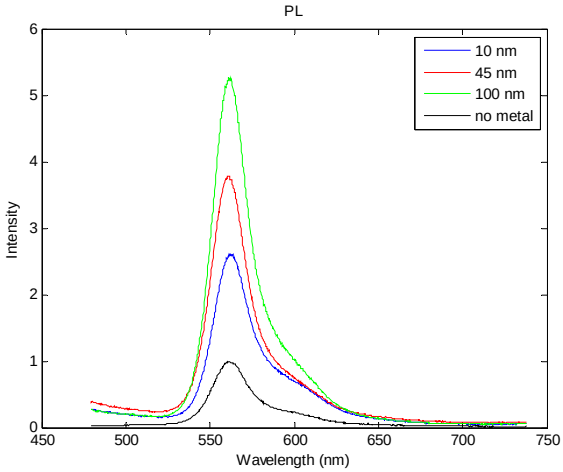

Figure 4.3. Photoluminescence intensity for silver coated samples with an emitter of 560 nm. Different spacer thicknesses were compared.

An enhancement on the intensity of 5,4 has been reported for silver.

To further investigate the wavelength dependency of the enhancement, which should be different with different metals, we divide the PL with metal at different distances with PL without metal. In pictures 4.4 and 4.5 we can see the PL enhancement ratio depending on the wavelength for samples coated with silver and gold and an emitter of 560 nm, respectively:

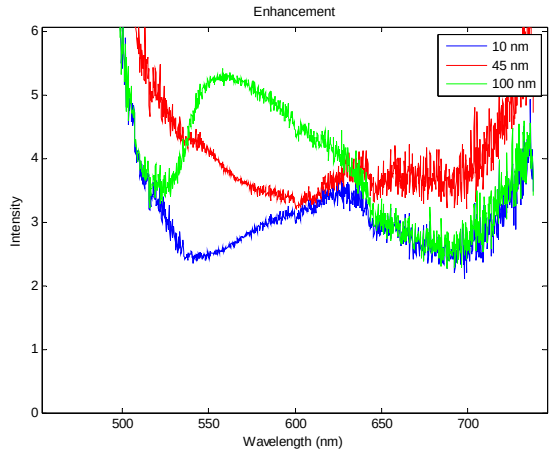

Figure 4.4. Enhancement ratio for silver coated samples and an emitter of 560 nm. Different spacer thicknesses were compared

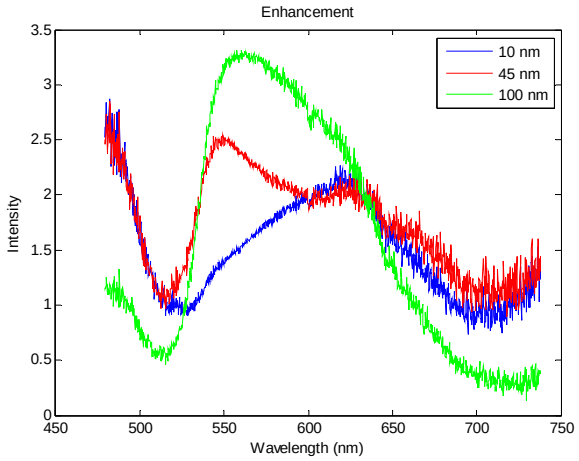

Figure 4.5. Enhancement ratio for gold coated samples and an emitter of 560 nm. Different spacer thicknesses were compared

As it has been mentioned before, the Plasmon frequencies of gold and silver are 650 nm and 558 nm, respectively [37]. The emissions of the fluorospheres are at 515 nm, 560 nm and 605 nm. Analyzing the absorption-emission spectra of the fluorospheres in figure 3.7, we could deduce that, for the same spacer thickness, the biggest coupling of light to SPPs would be with 605 nm emitter for gold and with 560 nm emitter for silver. The nearer the emission wavelength to the metal plasma frequency, the greater coupling to SPPs modes is presented.

We can see that the wavelength dependent enhancement ratio profile for both samples in figures 4.4 and 4.5 are very similar, although a greater enhancement is observed for silver. From this, we can deduce that our enhancement is not due to SPPs. If the enhancement was caused by SPPs, there would be a difference between both metals as they have different wavelength behavior.

It is thought that these results are due to thin film effects. The difference on the enhancement intensity may be due to the reflection of the emitted waves. Silver's plasma frequency is found at 558 nm and gold's plasma frequency is at 650 nm. As it is known, light above plasma frequency is transmitted and light below plasma frequency is reflected. That is why more reflection of the emitted light is produced at the silver surface.

This is not a proof for PL enhancement and as discussed in chapter 2.1.3 we should analyze the PL lifetime.

4.2 Photoluminescence lifetime

The radiative lifetime of an excited electronic state is the lifetime that would be obtained if radiative decay via SE were the only mechanism for depopulating this state. The rate of SE (and thus the lifetime of the excited level) is determined both by the properties of the atom and by the mode structure of the surrounding medium [38].

Starting from the PL decay curve, the lifetime can be calculated. It is built from a histogram which shows the distribution of arrival times of single photons after many excitation-detection cycles. In the simplest case, its result is a negative mono-exponential function that, while plotted on semi-logarithmical axes, results in a straight line [39].

The luminescence lifetime τ is related to the rate constants for radiative (k_R) and non radiative (k_{NR}) decay by:

$$\frac{1}{\tau} = k_{NR} + k_R \qquad (4.6)$$

Where the radiative lifetime is $1/k_R$ and the non radiative lifetime is $(1/k_{NR})$.

However, interference, caused by thin films, also affects the radiative lifetime of the emissive species as a function of wavelength.

The system showed in the picture 4.6 has been built to measure the PL decay ratio.

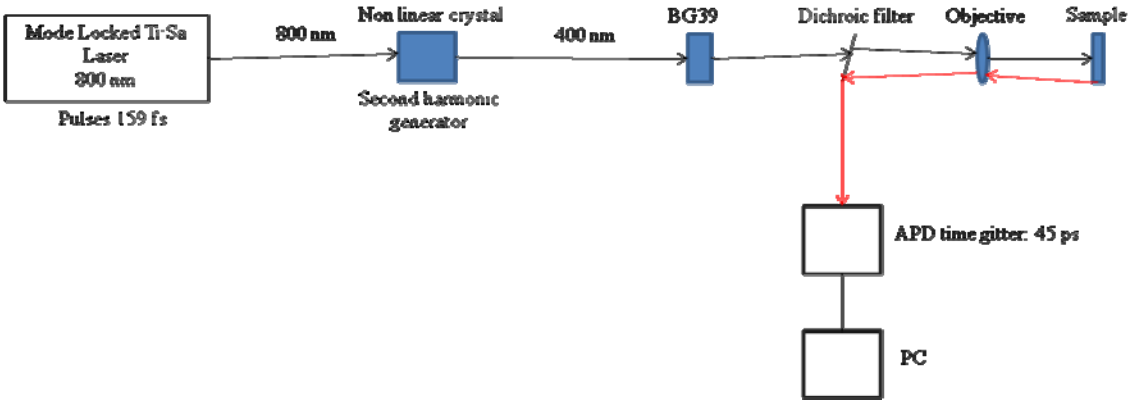

Figure 4.6. Lifetime measurement setup

A dichroic filter is a kind of filter that allows the transmission of certain frequencies and avoids the transmission of other frequencies by reflecting them. They are built by a superposition of different layers over a glass substrate, reinforcing certain wavelengths of light and interfering with other wavelengths. Every layer allows the pass of some wavelengths [40].

An avalanche photo diode (APD) has been used to detect the single photons emitted and then calculate the lifetime. The method used is time correlated single photon counting. It is based on the fact that for low level, high repetition rate signals the light intensity is usually low enough that the probability to detect more than one photon in one signal period is negligible. Individual photons are detected in different periods of the signal. The arrival time of the photon in the period is measured. After many periods, the detected photons are added for every time and then the distribution of the photon probability obtained.

After processing these data in the computer, it has been plot with semilogaritmical axes. The result silver and gold coated samples an emitter of 560 nm are shown in pictures 4.7 and 4.8, respectively:

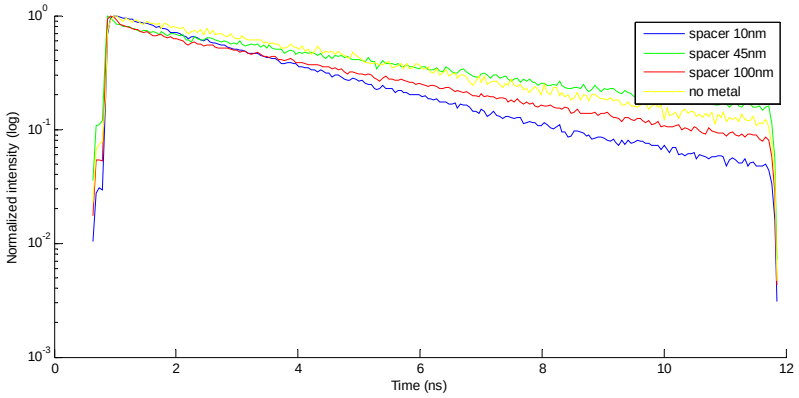

Figure 4.7. Photoluminescence lifetime for silver coated samples and an emitter of 560 nm. Different spacer thicknesses were compared.

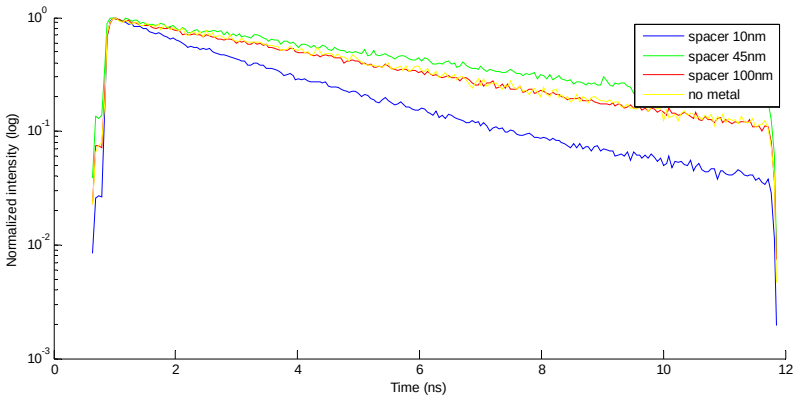

Figure 4.8. Photoluminescence lifetime for gold coated samples and an emitter of 560 nm. Different spacer thicknesses were compared.

It is seen for both metals that the shorter photoluminescence lifetime is found for the 10 nm thick spacer layer. The nearer the emitter is to the spacer layer, the better coupling of the emission to SPPs is found. So, the enhancement in SE rate will be bigger for small spacer thicknesses. As it was mentioned, the SE rate is inversely proportional to the photoluminescence lifetime. So, in pictures 4.7 and 4.8 the expected results are accomplished.

However, it is seen that photoluminescence lifetime for samples with a 100 nm thick spacer layer is shorter than lifetime for samples with a 45 nm thick spacer layer. This result disappoints with what has been told. As happened with the photoluminescence intensity results, it is thought that this fact may be due to thin film

effects. The measurements for the rest of the samples are not included here because they are similar to the results obtained for the samples analyzed in this text. However, they are shown in the appendix.

Due to the not satisfying results obtained, it was thought that maybe there was some kind of error in the samples production. So, in order to be sure of the results, it was decided to prepare a new set of samples using the same production method. Then the same PL measurements were repeated with the new samples and it was found that they were very similar to those done before, so we could conclude that the fabrication method was correct and that our samples were reproducible, both very important facts.

In figure 4.9 results of photoluminescence intensity and enhancement ratio for gold coated samples with an emitter of 560 nm thick are shown for both sets of samples. It is seen that the results are very similar for both charges and so it is deduced that the fabrication and measurement methods are correct.

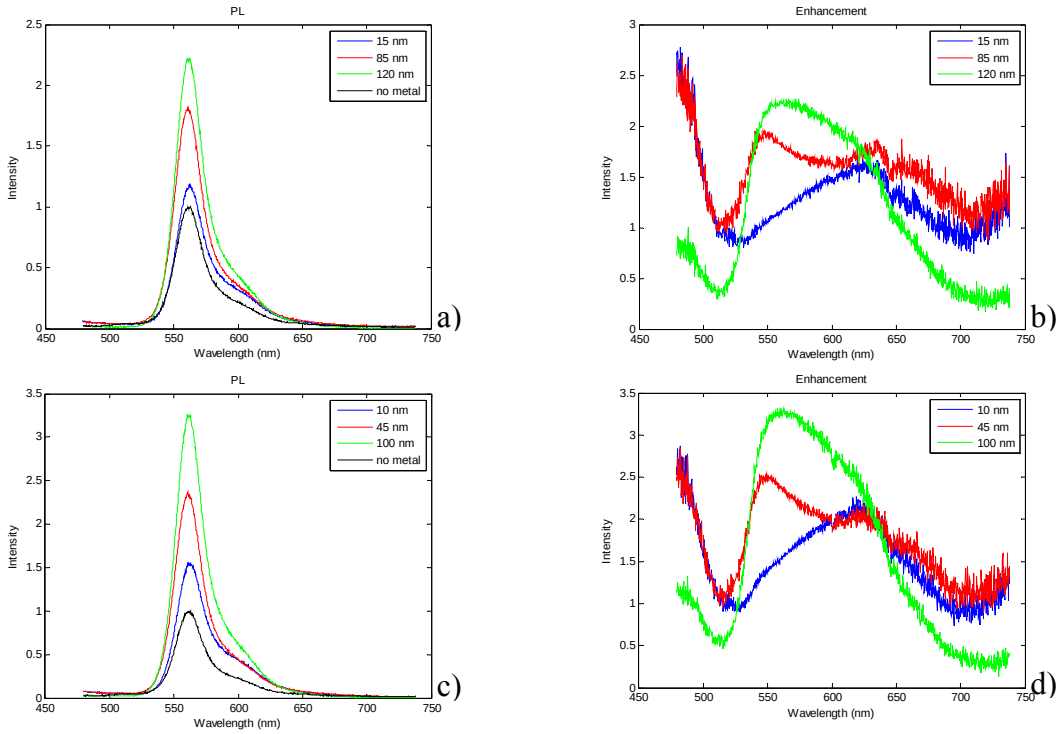

Figure 4.9. Photoluminescence intensity (a) and enhancement (b) measurements for a gold coated sample with an emitter of 560 nm thick spacer layer. The same measurements are shown for the second set of samples (c and d)

4.3 Simulation

A Finite Difference Time Domain (FDTD) simulation has been done with the software Lumerical.

The FDTD method is used to theoretically analyze electromagnetic fields within metal clad microcavities. The standard FDTD is based on Yee algorithm and solves directly Maxwell's time dependent curl equations:

$$\nabla \times \mathbf{E} = -\mu_0 \frac{\partial \mathbf{H}}{\partial t} \qquad (4.1)$$

$$\nabla \times \mathbf{H} = \varepsilon_0 \varepsilon_r \frac{\partial \mathbf{E}}{\partial t} \qquad (4.2)$$

So that both space and time have to be discretized.

But when working with metals at optical frequencies some changes to the standard Yee's FDTD scheme have to be done. Electromagnetic fields in metals are described by adding a current term to Maxwell's curl equations (Drude model).

$$\nabla \times \mathbf{E} = -\mu_0 \frac{\partial \mathbf{H}}{\partial t} \qquad (4.3)$$

$$\nabla \times \mathbf{H} = \varepsilon_0 \varepsilon_r \frac{\partial \mathbf{E}}{\partial t} + \mathbf{J} \qquad (4.4)$$

$$\frac{\partial \mathbf{J}}{\partial t} + \nu \mathbf{J} = \varepsilon_0 \omega_p^2 \mathbf{E} \qquad (4.5)$$

Where ω_p is the plasma frequency of a metal and υ is the corresponding damping rate [41-42].

The designed layout for this measurement is shown in picture 4.10.

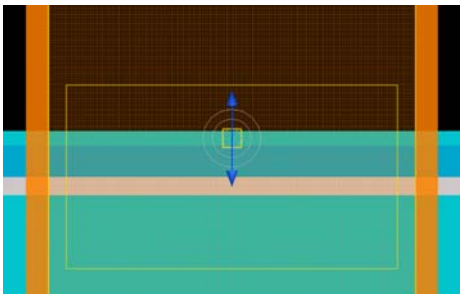

Figure 4.10. Designed layout for Lumerical simulations

The result is shown in picture 4.11, where it can be clearly seen the similarity between the real measurement and simulation. The real measurement corresponds to a silver coated sample with a spacer thickness of 15 nm and an emitter of 560 nm while in the simulation the spacer thickness is 20 nm.

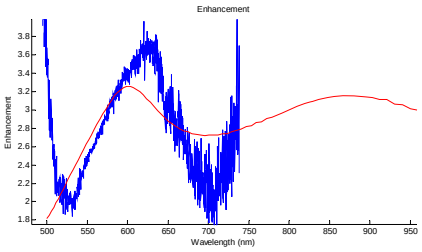

Figure 4.11. Enhancement ratio for silver coated sample with a 15 nm thick spacer layer and an emitter with 560 nm wavelength (blue line) is compared to a Lumerical simulation for silver coated sample with a 20 nm thick spacer layer and an emitter with 560 nm wavelength (red line).

A possible reason that explains the unexpected behavior of our samples is the existence of interferences between the directly emitted waves and the waves reflected from the metal layer. The effect of interference on the radiative properties of an excited molecule is dependent on the emission wavelength, and this wavelength dependence is a function of the distance between the emitter and the metal [43]. Another important fact that influences the emitting properties is the energy transfer to the metal [44-46].

So, the measured PL is an addition of some factors. First of all, the own emission from fluorospheres due to the laser excitation, but also that emission due to the reflected emission. However, this fact is not very important as it can be seen from the

absorption-emission spectrum of the emitters in figure 3.7 (there is almost no overlapping between both spectrums). The laser light is also reflected on the metal surface and this reflected light excites the fluorospheres leading to different pump of the emitters. We can also find the enhanced emission light scattered out of the metal due to SPPs and the reflection on the metal's surface of both the pump light and the emitting light, leading to some wavelengths interferences.

5 Outlook and conclusion

An enhancement on photoluminescence was observed for metal coated samples with an emitter separated by the metal with a spacer layer. The coupling to SPPs is better when the emitter is placed at small distances from the metal. So, a bigger enhancement ratio should be observed for small spacer thicknesses. However, the obtained results show a disappointment with the expected ones.

Photoluminescence lifetime is inversely proportional to the spontaneous emission ratio. So, additional photoluminescence lifetime measurements have been done. The lower lifetime was obtained for the thinner spacer layer. However, the corresponding lifetimes for the rest of spacer layer thicknesses did not follow the expected behavior.

It has been seen that enhancement in photoluminescence depends on the metal used and the spacer thickness. Better enhancements have been found for silver coated samples than for gold coated samples. This is because silver's surface is rougher than gold's surface and it may scatter out SPPs better than gold. The difference in enhancement is also due to the different plasma frequencies of both metals. Silver's plasma frequency is higher than gold's one and so, silver reflects more emitted light than gold. This fact also affects the enhancement on photoluminescence intensity.

So, it has been thought that the photoluminescence intensity's observed enhancement may be due to the coupling of the emission to surface Plasmon polaritons modes or due to thin film effects caused by the metal surface. Further studies should be done to understand it.

6 Appendix

6.1 Matlab files

6.1.1 Photoluminescence

```
%%It compares photoluminescence of different materials with certain
%%spacer and emitter

Pfad = uigetdir;
%Opens the actual directory

%Data importation
Dat0 = importdata([Pfad '\data1.dat'], '\t', 32);
Dat1 = importdata([Pfad '\data2.dat'], '\t', 32);
Dat2 = importdata([Pfad '\data3.dat'], '\t', 32);
Dat3 = importdata([Pfad '\data4.dat'], '\t', 32);
Dat4 = importdata([Pfad '\dark_5sec.dat'], '\t', 32);

%It equals the different scales used for the different measurements
a=5/5;
b=5/5;
c=5/5;
d=5/5;

data_all(:,1) = Dat0.data(:,1);
data_all(:,2) = Dat0.data(:,2)*a-Dat4.data(:,2);
data_all(:,3) = Dat1.data(:,2)*b-Dat4.data(:,2);
data_all(:,4) = Dat2.data(:,2)*c-Dat4.data(:,2);
data_all(:,5) = Dat3.data(:,2)*d-Dat4.data(:,2);


%Normalization to the uncoated sample
e=max(data_all(:,5));

data_all(:,2) = data_all(:,2)/e;
data_all(:,3) = data_all(:,3)/e;
data_all(:,4) = data_all(:,4)/e;
data_all(:,5) = data_all(:,5)/e;


%It substracts 35 to frequency to correct spectrometer error

for i=1:1024
    data_all(i,1)=data_all(i,1)-135;
end

disp('READING DATA FROM FILE... COMPLETE') %%% Display output %%%


%it draws all graphics together
figure;
hold on;
plot(data_all(:,1),data_all(:,2));  %spacer 10 nm
plot(data_all(:,1),data_all(:,3), 'r'); %spacer 45 nm
plot(data_all(:,1),data_all(:,4), 'g'); %spacer 100 nm
```

```
plot(data_all(:,1),data_all(:,4), 'g'); %no metal
```

6.1.2 Enhancement ratio

```
Pfad = uigetdir;
%Opens the actual directory

%Data importation
Dat0 = importdata([Pfad '\data1.dat'], '\t', 32);
Dat1 = importdata([Pfad '\data2.dat'], '\t', 32);
Dat2 = importdata([Pfad '\data3.dat'], '\t', 32);
Dat3 = importdata([Pfad '\data4.dat'], '\t', 32);
Dat4 = importdata([Pfad '\dark_5sec.dat'], '\t', 32);

%It equals the different scales used for the different measurements
a=5/5;
b=5/5;
c=5/5;
d=5/5;

data_all(:,1) = Dat0.data(:,1);
data_all(:,2) = Dat0.data(:,2)*a-Dat4.data(:,2);
data_all(:,3) = Dat1.data(:,2)*b-Dat4.data(:,2);
data_all(:,4) = Dat2.data(:,2)*c-Dat4.data(:,2);
data_all(:,5) = Dat3.data(:,2)*d-Dat4.data(:,2);


%Normalization to the uncoated sample
e=max(data_all(:,5));

data_all(:,2) = data_all(:,2)/e;
data_all(:,3) = data_all(:,3)/e;
data_all(:,4) = data_all(:,4)/e;
data_all(:,5) = data_all(:,5)/e;


%It substracts 35 to frequency to correct spectrometer error

for i=1:1024
    data_all(i,1)=data_all(i,1)-135;
end

disp('READING DATA FROM FILE... COMPLETE') %%% Display output %%%

%it draws all graphics together
figure;
hold on;
plot(data_all(:,1),(data_all(:,2)./data_all(:,5))); %10 nm spacer
plot(data_all(:,1),(data_all(:,3)./data_all(:,5)), 'r'); %45 nm spacer
plot(data_all(:,1),(data_all(:,4)./data_all(:,5)), 'r');%100 nm spacer
```

6.1.3 Lifetime

```
clear all;

Dat0 = importdata(['data1.asc']);
Dat1 = importdata(['data2.asc']);
```

```
Dat2 = importdata(['data3.asc']);
Dat3 = importdata(['data4.asc']);

data_all(:,2) = Dat0(:,1); %intensity
data_all(:,3) = Dat1(:,1);
data_all(:,4) = Dat2(:,1);
data_all(:,5) = Dat3(:,1);

a = max(data_all(:,2));
b = max(data_all(:,3));
c = max(data_all(:,4));
d = max(data_all(:,5));

data_all(:,1)=0:(12.5/(256-1)):12.5;

disp('READING DATA FROM FILE... COMPLETE') %%% Display output %%%

figure;
hold on;

plot(data_all(1:256,1),(data_all(1:256,2)/a), 'b');  %spacer 10nm
plot(data_all(1:256,1),(data_all(1:256,3)/b), 'g');  %spacer 45nm
plot(data_all(1:256,1),(data_all(1:256,4)/c), 'r');  %spacer 100nm
plot(data_all(1:256,1),(data_all(1:256,5)/d), 'y');  %no metal
```

6.2 Measurements

The photoluminescence intensity, enhancement ratio and lifetime plots for the samples that were not shown in chapter 4 are shown in the following pictures. The reached conclusions are the same that for the samples shown in chapter 4.

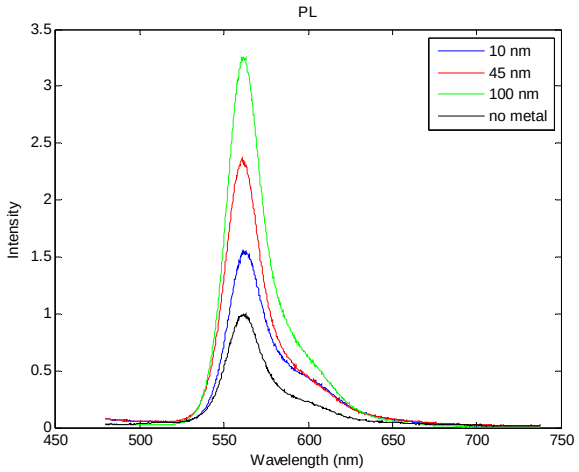

Figure 6.1. Photoluminescence intensity for gold coated samples with an emitter of 560 nm. Different spacer thicknesses were compared.

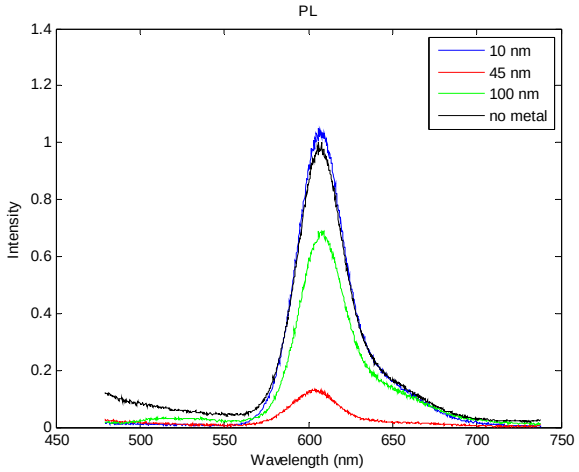

Figure 6.2. Photoluminescence intensity for gold coated samples with an emitter of 605 nm. Different spacer thicknesses were compared.

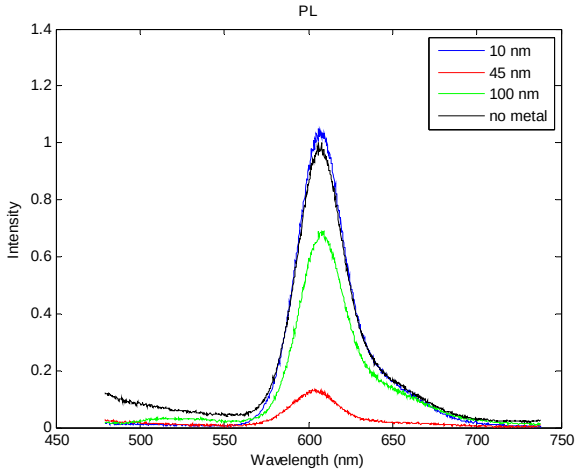

Figure 6.3. Photoluminescence intensity for silver coated samples with an emitter of 605 nm. Different spacer thicknesses were compared.

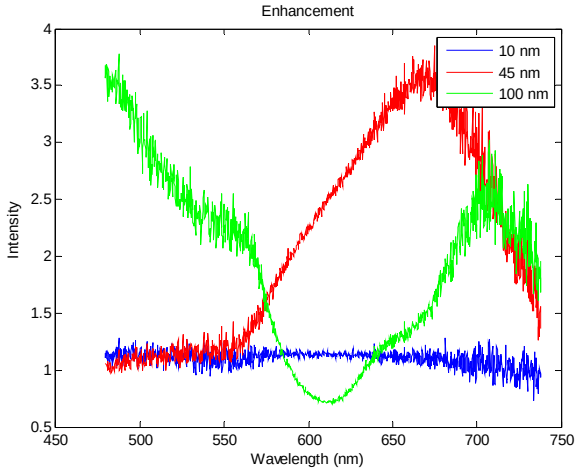

Figure 6.4. Enhancement ratio for silver coated samples and an emitter of 605 nm. Different spacer thicknesses were compared

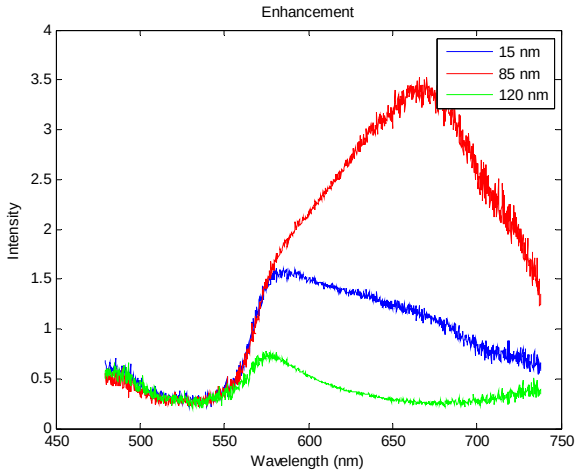

Figure 6.5. Enhancement ratio for gold coated samples and an emitter of 605 nm. Different spacer thicknesses were compared

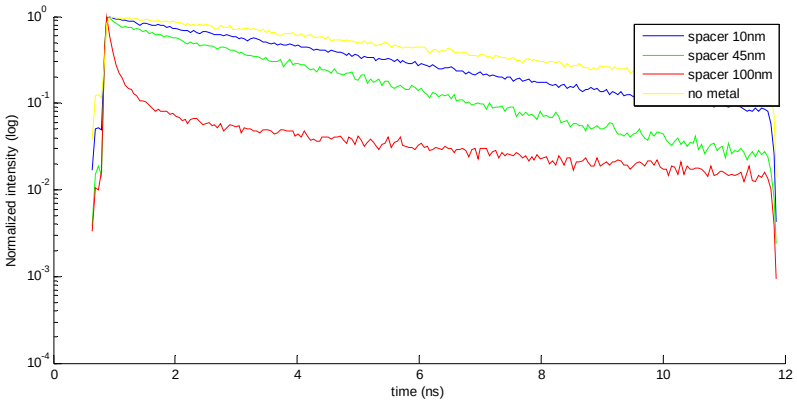

Figure 6.6. Photoluminescence lifetime for silver coated samples and an emitter of 605 nm. Different spacer thicknesses were compared.

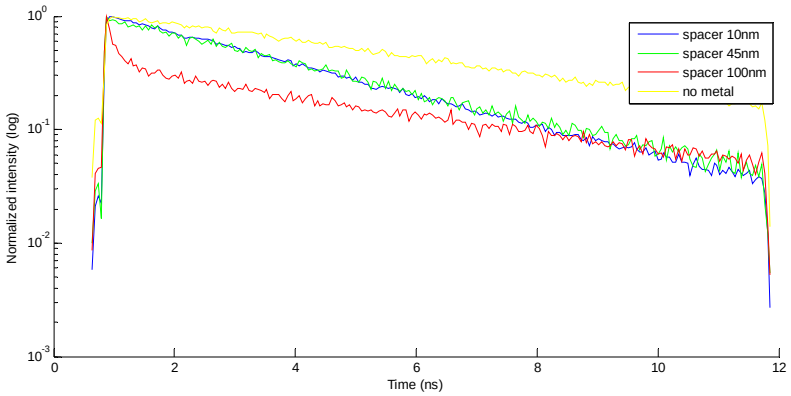

Figure 6.7. Photoluminescence lifetime for gold coated samples and an emitter of 605 nm. Different spacer thicknesses were compared.

References

1. Y. A. ONO, *ELECTROLUMINESCENCE IN ENCYCLOPEDIA OF APPLIED PHYSICS*, ED. G. L. TRIGG, VCH, WEINHEIM, VOL. 5, P. 295. 1993.
2. G. Destriau, *Journal of Chemical Physics*, 33, 587. 1936.
3. N. Holonyak Jr and S. F. Bevacqua, *Applied Physics Letters*, 1, 82. 1962.
4. M. Pope, H. P. Kallmann and P. Magnante, *Journal of Chemical Physics*, 38, 2042. 1963.
5. W. Helfrich and W. G. Schneider, *Physical Review Letters*, 14, 229. 1965.
6. A. Kraft, A. C. Grimsdale and A. B. Holmes, *Angewandte Chemie, Int. Ed.*, 37, 402. 1998.
7. S. Tasch, W. Graupner, G. Leising, L. Pu, M. W. Wagner and R. H. Grubbs, *Advanced Materials*, 7, 903. 1995.
8. http://electronics.howstuffworks.com/oled1.htm
9. www.olla-project.org
10. *The hand book-A Guide to fluorescent Probes and Labelling Technologies*, 10th edition, http://probes.invitrogen.com/handbook/.
11. http://en.wikipedia.org/wiki/Spontaneous_*emission*
12. S. Noda, M. Fujita and T. Asano. *Spontaneous-emission control by photonic crystals and nanocavities*. Nature Photonics, vol. 1, 2007.
13. http://en.wikipedia.org/wiki/Smith-Purcell_effect
14. H. Ditlbacher, J. R. Krenn, G. Schider, A. Leitner and F. R. Aussenegg, *Two-dimensional optics with surface plasmon polaritons*, Applied Physics Letters, vol. 81, num. 10. 2002.
15. W. L. Barnes, A. Dereux and T. W. Ebbesen, *Surface plasmon subwavelength optics*. Nature, vol. 424. 2003.
16. G. Winter, W. A. Murray, S. Wedge and W. L. Barnes. *Spontaneous emission from within a metal-clad cavity mediated by coupled surface plasmon-polaritons*. Journal of Physics: Condensed Matter, 20. 2008.
17. W. H. Weber and C. F. Eagen, *Energy transfer from an excited dye molecule to the surface plasmons of an adjacent metal*. Optics Letters, 4, 236-238. 1979.

18. I. Pockrand, A. Brillante and D. Möbius. *Nonradiative decay of excited molecules near a metal surface*. Chemical Physics Letters, 69, 499-504.
19. W. L. Barnes. *Fluorescence near interfaces: the role of photonic mode density*. Journal of Modern Optics, 45, 661-699. 1998.
20. P. A. Hobson, S. Wedge, J. A. E. Wasey, I. Sage and W. L. Barnes. *Surface plasmon mediated emission from organic light emitting diodes*. Advanced Materials, 14, 1393-1396. 2002.
21. U. Kreibig and M. Vollmer. *Optical properties of metal clusters*. Springer, Berlin. 1995.
22. *Special Issue: Optical Properties of Nanoparticles*. Applied Physics, B73. 2001.
23. C. L. Haynes and R. P. Van Duyne. *Nanosphere lithography: A versatile nanofabrication tool for studies of size-dependent nanoparticle optics*. Journal of Physical Chemistry, B105, 5599-5611. 2001.
24. C. Sonnichsen et al. *Spectroscopy of single metallic nanoparticles using total internal reflection microscopy*. Applied Physics Letters, 77, 2949-2951. 2000.
25. http://www.lrsm.upenn.edu/~frenchrh/mie_scattering.htm
26. http://www.beckmancoulter.com/coultercounter/homepage_tech_mie.jsp
27. http://hyperphysics.phy-astr.gsu.edu/Hbase/atmos/blusky.html
28. H. Schade and Z. E. Smith. *Mie scattering and rough surfaces*. Applied optics, volume 24, number 19. 1985.
29. http://www.plasma.de/en/index.html
30. K. Okamoto, I. Niki, A. Shvartser, Y. Narukawa, T. Mukai, A. Scherer. Nat. Mater., 3, 601. 2004.
31. D. K. Gifford, D. G. Hall. Applied Physics Letters, 80, 3679. 2002.
32. X. Wu, M. H. Chowdhury, C. D. Geddes, K. Aslan, R. Domszy, J. R. Lakowicz, A. J.-M. Yang. Thin Solid Films, Volume 516, Issue 8, Pages 1977-1983. 2008.
33. V. Reboud, N. Kehagias, M. Zelsmann, C. Schuster, M. Fink, F. Reuther, G. Gruetzner and C. M. Sotomayor Torres. *Photoluminescense enhancement in nanoimprinted photonic crystals and coupled surface plasmons*, Optics Express 7190, Vol. 15, No. 12. 2007.
34. http://www.redoptronics.com/nonlinear-crystals.html

35. http://www.rp-photonics.com/nonlinear_crystal_materials.html
36. http://www.besoptics.com/html/body_schott_bg39_filter_glass.html
37. V. Reboud, N. Kehagias, M. Zelsmann, C. Schuster, M. Fink, F. Reuther, G. Gruetzner and C. M. Sotomayor Torres. *Photoluminescence enhancement in nanoimprinted photonic crystals and coupled surface plasmons*. Optics Express 7190. Vol. 15, No. 12. 2007.
38. http://www.rp-photonics.com/radiative_lifetime.html
39. http://en.wikipedia.org/wiki/Spontaneous_emission
40. http://en.wikipedia.org/wiki/Dichroic_filter
41. M. L. Brongersma, P. G. Kik (Editors), *Surface Plasmon Nanophotonics*, Springer Series in Optical Sciences. Springer. 2007.
42. J. Vučković, M. Lončar and A. Scherer. *Surface Plasmon Enhanced Light-Emitting Diode*, IEEE Journal of Quantum Electronics, vol. 36, no. 10. 2000.
43. H. Becker, S. E. Burns and R. H. Friend, *Effect of metal films on the photoluminescence and electroluminescence of conjugated polymers.* Physical Review B, volume 56, number 4. 1997.
44. H. Kuhn. Journal of Chemical Physics, 53, 101. 1970.
45. K. H. Drexhage, in *Progress in optics*, edited by E. Wolf. North-Holland, Amsterdam. Pp. 163-232. 1974.
46. R. R. Chance, A. Prock, and R. Silbey. Advances in Chemical Physics. 37, 1 . 1978.

Acknowledgements

First of all I want to thank to my supervisor Yousef, who has helped me a lot and, even being on holidays, has been answering all my questions.

I want also thank Prof. Dr. Uli Lemmer, for giving me the chance to work in his team and the good ideas and discussions.

To Klaus and Thorsten for showing me the secrets of the work in the clean room.

To all my LTI colleagues for they support and good times.

And finally to my family and friends, that have understood me in the last days of my thesis even I did not have much time for them.